Prof. Sergiy Kotrechko
G.V. Kurdyumov Institute for Metal Physics of NAS of Ukraine
serkotr@gmail.com

IRRADIATION EMBRITTLEMENT AND RPV METAL SERVICE LIFE: STATE-OF-THE-ART AND CHALLENGES

Age Distribution of Operating Nuclear Power Reactors

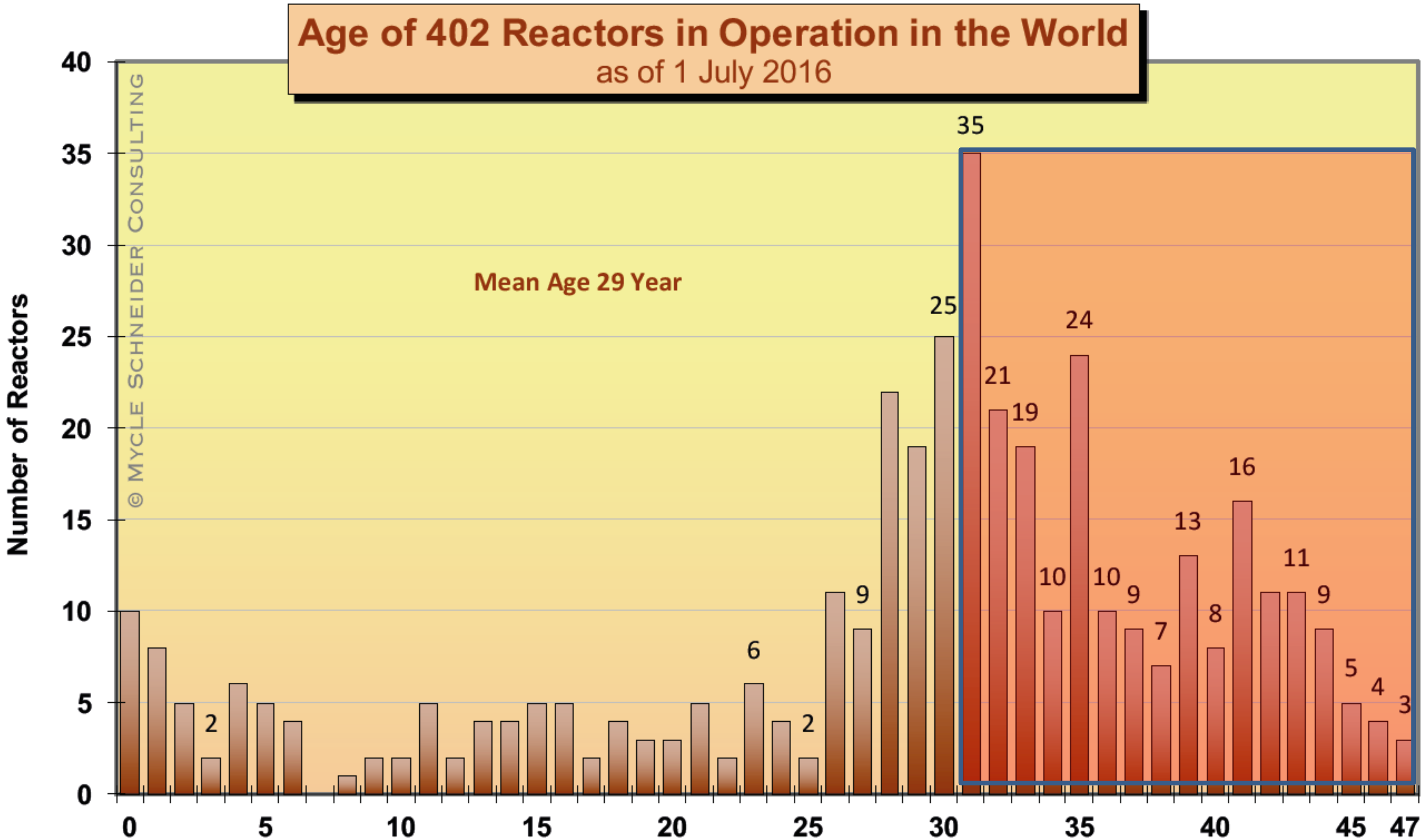

Source:The World Nuclear Industry Status Report 2016
https://www.worldnuclearreport.org

The **aim** of the report is to summarize the state of knowledge on the two key components of this issue, namely:

- micromechanisms of radiation embrittlement of RPV metal with an emphasis on the high fluences;
- modern approaches to RPV-lifetime prediction

Outline of presentation

1. Introduction.

2. Radiation embrittlement of RPV metal.

2.1. Micromechanisms of radiation hardening.

2.2. Brittle strength of irradiated metal.

3. Prediction of the end-of-life fluence for the reactor pressu vessel.

3.1. Engineering approach.

3.2. Physically-based approaches to lifetime prediction.

4. Radiation-induced softening.

5. Conclusions and open issues.

Radiation defects

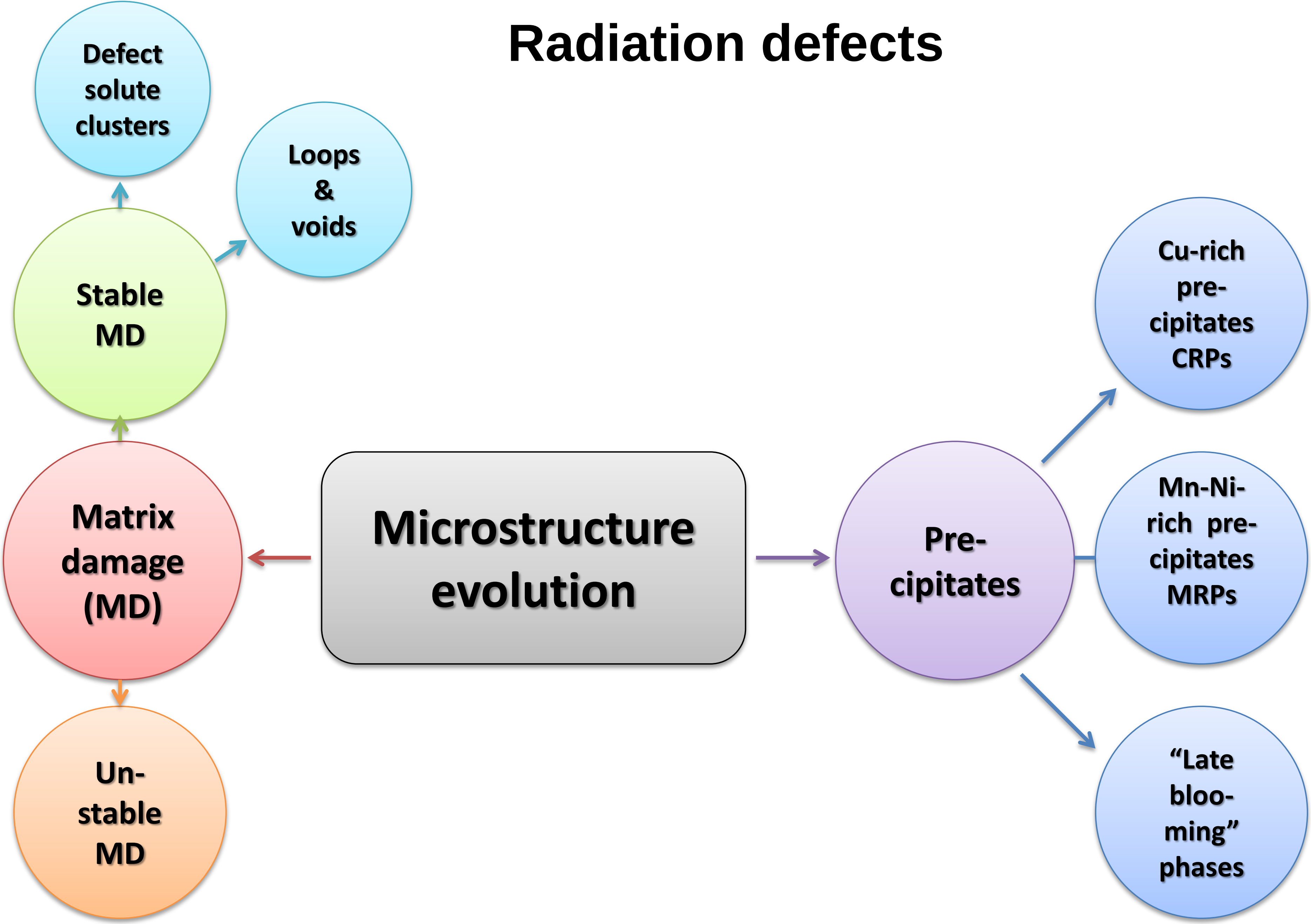

Microstructure features evolution

Solute fluctuation → **Solute-enriched clusters** → **Precipitate**

Fluence increasing →

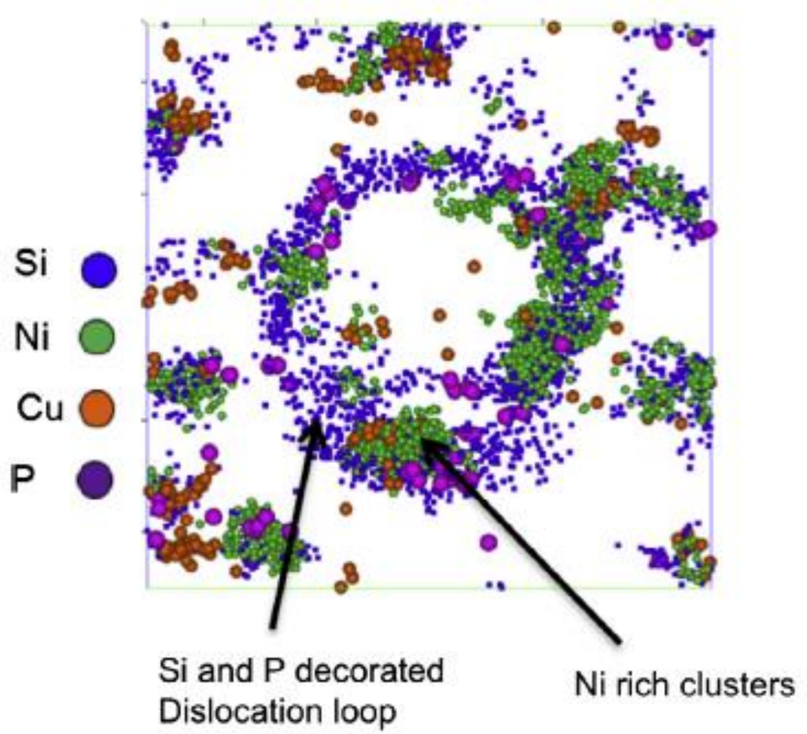

Loops can act as nucleation sites for the formation of atomic segregations. Subsequently, they can convert into precipitates.

E. A. Marquis et al. Current Opinion in Solid State and Materials Science 17 (2013) 217-223.

Effect of Mn, Ni and Cu segregated around the dislocation loop on resistance to dislocation move

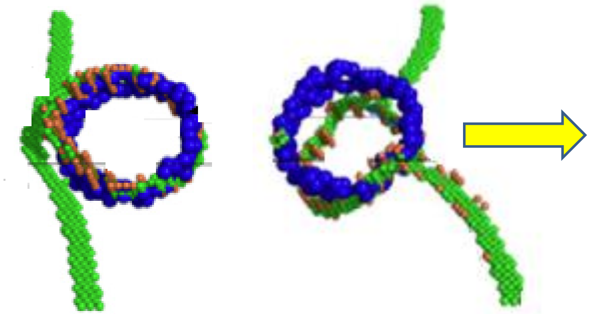

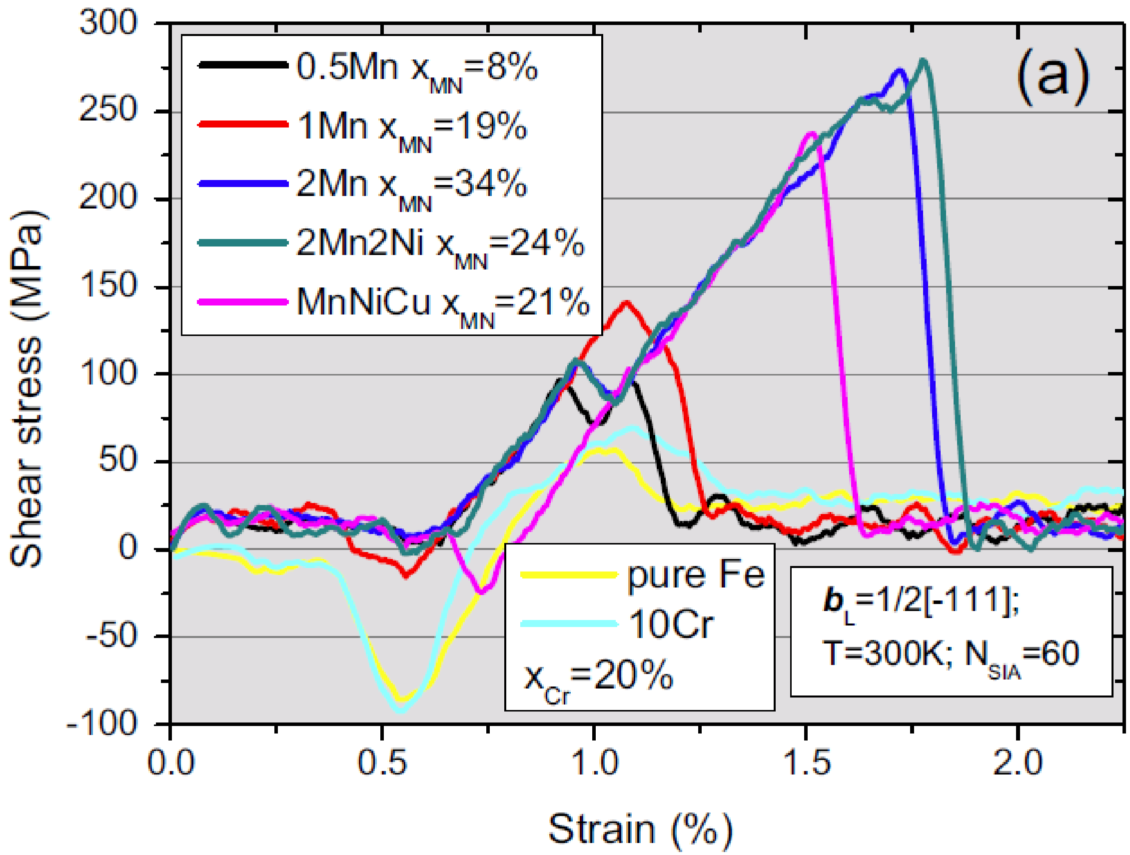

Stress–strain relationship corresponding to the interaction of a_0/2 [111] DLs of size 1.5 nm

D. Terentyev, X. Heb, G. Bonny, A. Bakaev, E. Zhurkin, L. Malerba
Journal of Nuclear Materials 457(2015) 173-181

Radiation hardening as a collective process

MD-simulation - details of the interaction of a dislocation with a separate obstacle.

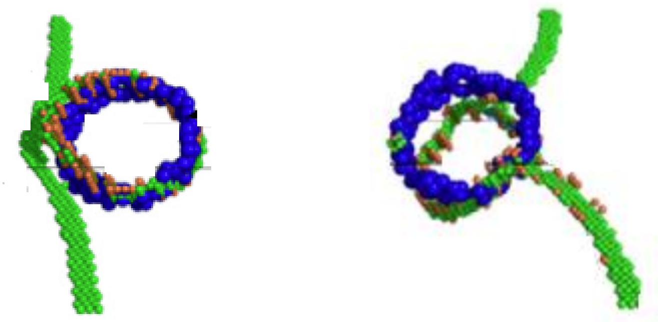

Dislocation dynamics – simulation of the stochastic process of interaction of dislocations with defects.

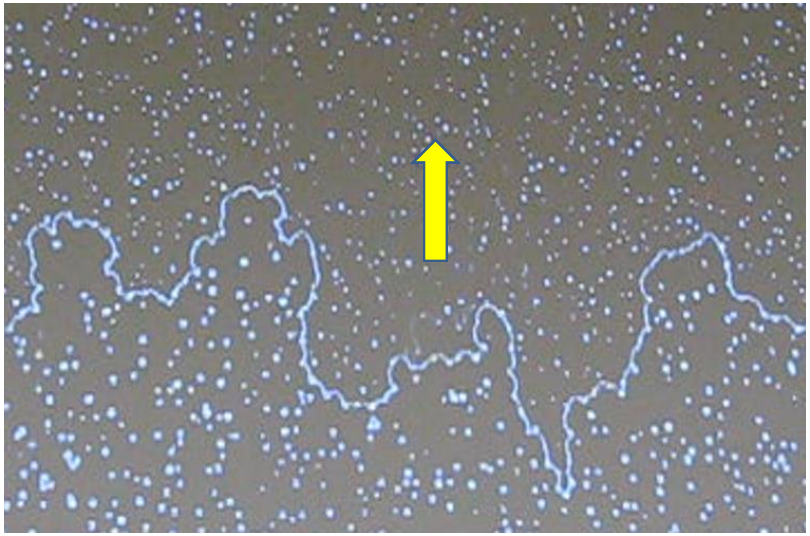

It is necessary to develop advanced models of radiation hardening taking into account both the properties of individual defects, and the collective processes of interaction of a moving dislocation with a field of defects.

D.J. Bacon, U.F. Kocks, R.O. Scattergood, Philos. Mag. 28 (1973) 1241–1263

Phenomenological approach

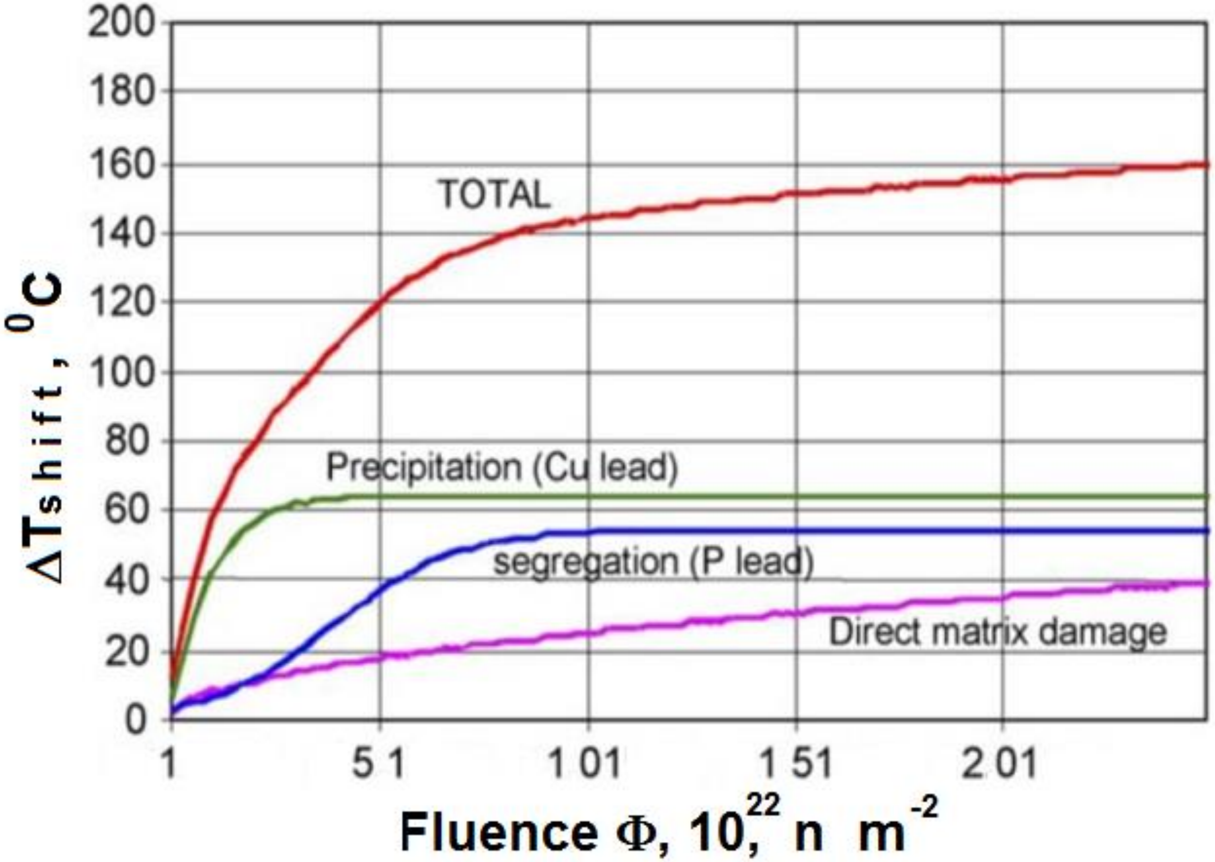

Matrix:

$$\Delta T_{sh} = \left[a\Phi^{1/2}\right]$$

Cu-precipitation:

$$\Delta T_{sh} = b\left[1 - \exp\left(-\frac{\Phi}{\Phi_{sat}}\right)\right]$$

P-segregation:

$$\Delta T_{sh} = \frac{c}{2}\left[1 - \tanh\left(-\frac{\Phi - \Phi_{segr}}{c2}\right)\right]$$

Debarberis L. et al. *International Journal of Pressure Vessels and Piping,* 82 195-200.

Late blooming effect

The ascertainment of differences in the regularities of radiation hardening in RPV-metals with a high and low (C < 0.05 - 0.07% Cu) content of copper is one of the important directions of activity in radiation materials science.

To date, the differences are often associated with the "**late blooming effect"**

Odette suggested (~1998) the existence of “**late blooming phases”** (LBPs).

Main features:

- **they have a long incubation period;**
- **they have rapid growth thereafter;**
- **they should be present in large volume fractions at equilibrium**.

These phases should be formed at high fluence preferably in low-Cu steels, which contain significant amounts of Ni and Mn.

Formation of this phase should result in **sudden severe** embrittlement, therefore, it can be dangerous for RPV under long time operation condition.

G. R. Odette and G. E. Lucas, Radiation Effects and Defects in Solids, 144 (1998) pp. 189-231

B. Radiguet et al., presented at “Longlife” Final International Workshop, 15-6 January 2014, Dresden (Germany).

L. Malerba, “Longlife” Final International Workshop, Dresden, 15-6 Jan 2014.

Late blooming phases

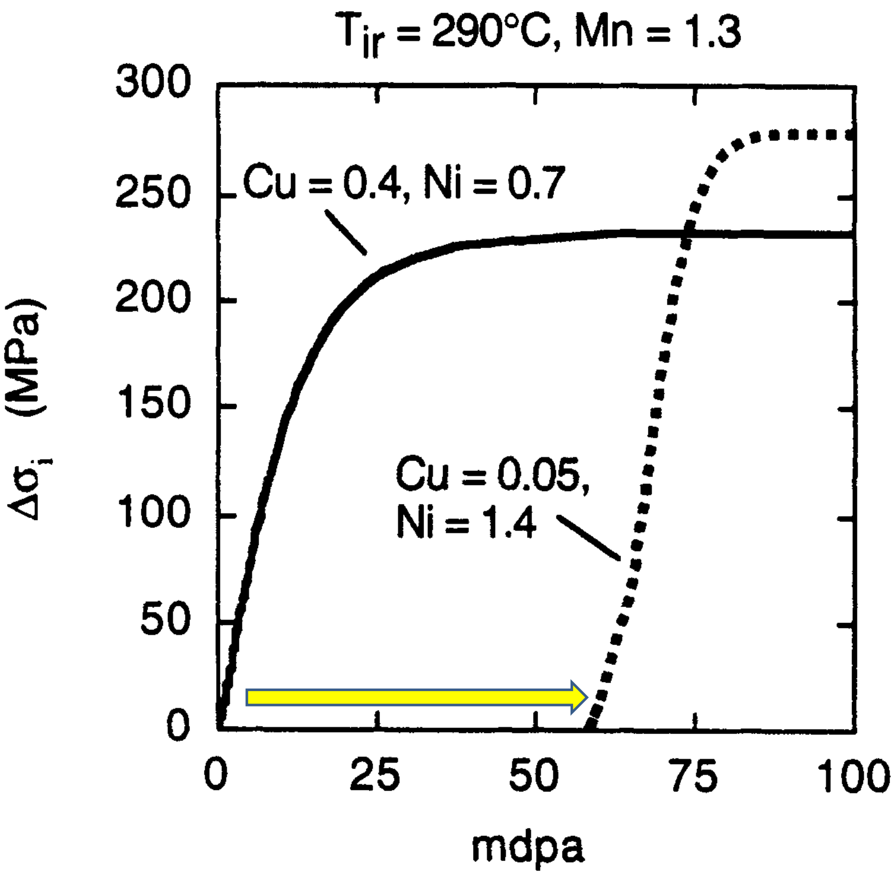

Outstanding issues:

•There are controversial viewpoints on the existence or not of "Blooming effect" and whether they are really "Blooming" or not.

•For low-Cu steels it is not clear whether there is an incubation period.

The predicted $\Delta\sigma_Y$ for a CRP-dominated microstructure in a high Cu / medium Ni steel compared to a MNP-dominated microstructure in a low Cu / high Ni steel with the incubation fluence increased by a factor of 200.

G.R. ODETTE and G.E. LUCAS Radiation Effects and Defects in Solids
Volume 144, 1998 – Issue 1-4

Acceleration of radiation hardening of low-copper RPV steels

Element	C	Si	Mn	S	P	Cr	Ni	Mo	V	Cu
A533B cl.1 (JPB) (wt%)	0.18	0.26	1.42	0.001	0.017	0.15	0.83	0.54	0.01	0.01
A533B cl.1 (JPC) (wt%)	0.18	0.27	1.45	0.002	0.007	0.15	0.81	0.54	0.01	0.01
A508 cl.1 (JFL) (wt%)	0.17	0.25	1.42	0.002	0.004	0.16	0.75	0.52	0.004	0.01

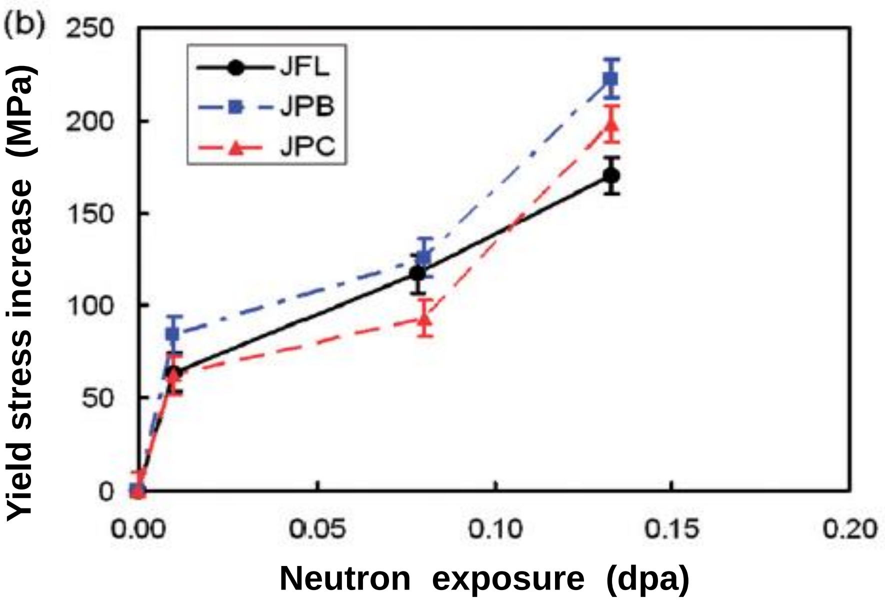

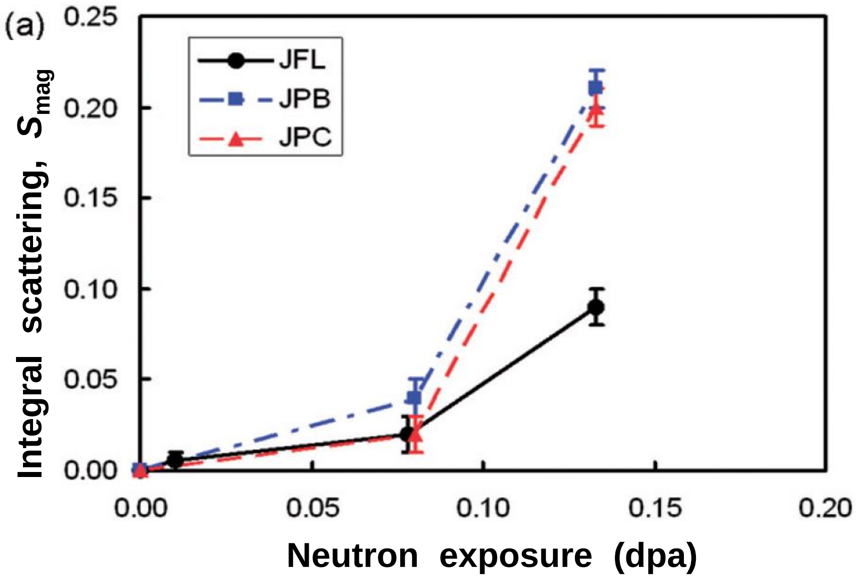

"The example of the reference RPV steel JFL (forging) as well as the low irradiation temperature of 255^{0}C indicates that the results obtained for JPB and JPC (plate) cannot be directly transferred to real operation conditions of RPVs. The practical implication of our result is rather to contribute to the specification of parameter fields defining conditions under which late blooming effect occurs or do not occur".

F. Bergner, A. Ulbricht and H.-W. Viehrig Phil. Mag. Letters Vol. 89, No. 12, December 2009, 795–805

High-nickel WWER-1000 base (15Kh2NMFAA) and weld (12Kh2N2MAA) metal

Element	C	Si	Mn	Cr	Ni	Cu	S	P	V	Mo
Base metal (wt%)	0.17	0.29	0.47	2.24	1.34	0.05	0.014	0.009	0.09	0.51
Weld metal (wt%)	0.08	0.26	0.74	1.80	1.77	0.07	0.013	0.006	0.02	0.64

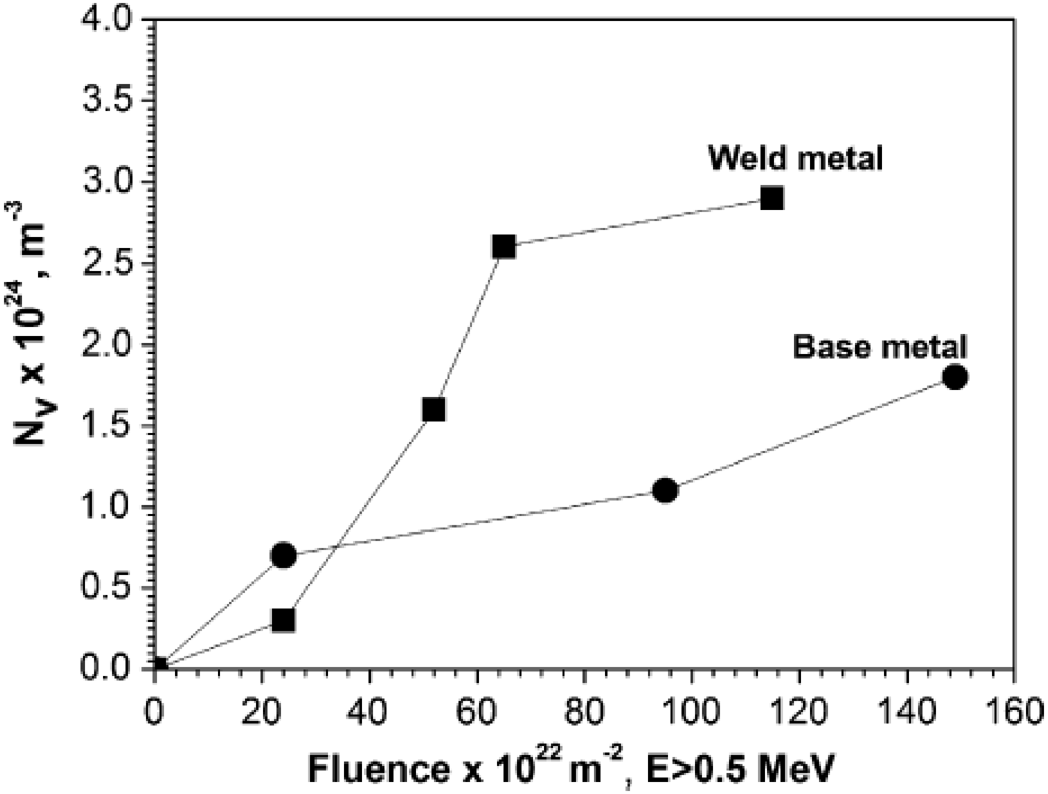

An increase in number density of the Ni-, Si- and Mn-enriched nanoclusters in the base and weld metals with fluence takes place, but they are not “late” and not “blooming”.

M.K. Miller et al Journal of Nuclear Materials 385 (2009) 615–622

Atomistic simulation

Kinetic of formation of MNPs must follow the kinetic of formation of dislocation loops:

- no sudden blooming is expected, but gradual accumulation of decorated loops with increasing dose;
- the conventional distinction between matrix damage and precipitates becomes blurred.

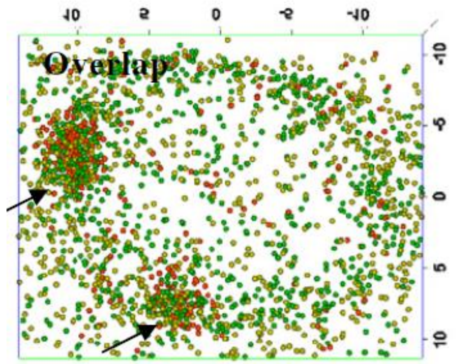

Z. Jiao, G.S. Was Acta Materialia 59 (2011) 4467-4481

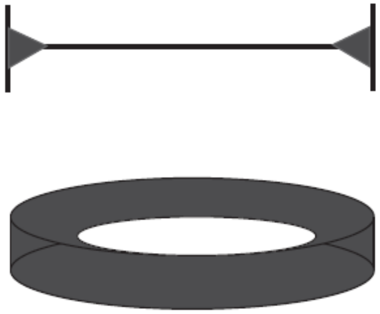

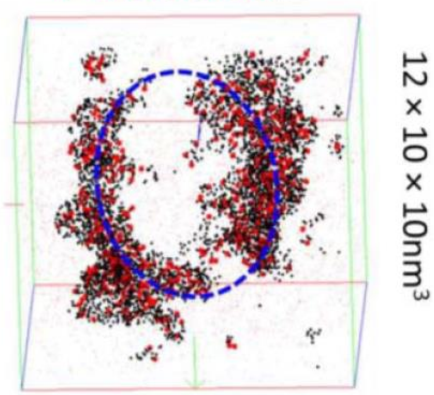

Solute atoms EDF 2 irradiated at $6.95{\times}10^{19}$n.cm^{-2}. *[B. Radiguet LONGLIFE D3.3]*

Altstadt, E. (2014). *LONGLIFE Final International Workshop, Dresden, Germany.*
Lorenzo Malerba *Longlife* Final International Workshop, Dresden, 15-16 Jan 2014
R. Ngayam-Happy, C.S. Becquart, C. Domain, L. Malerba, Journal of Nuclear Materials 426 (2012) 198.

Evolution of microstructure of WWER-1000 metal

BM (1.34%Ni, 0.47%Mn, 0.29%Si, 0.05%Cu)

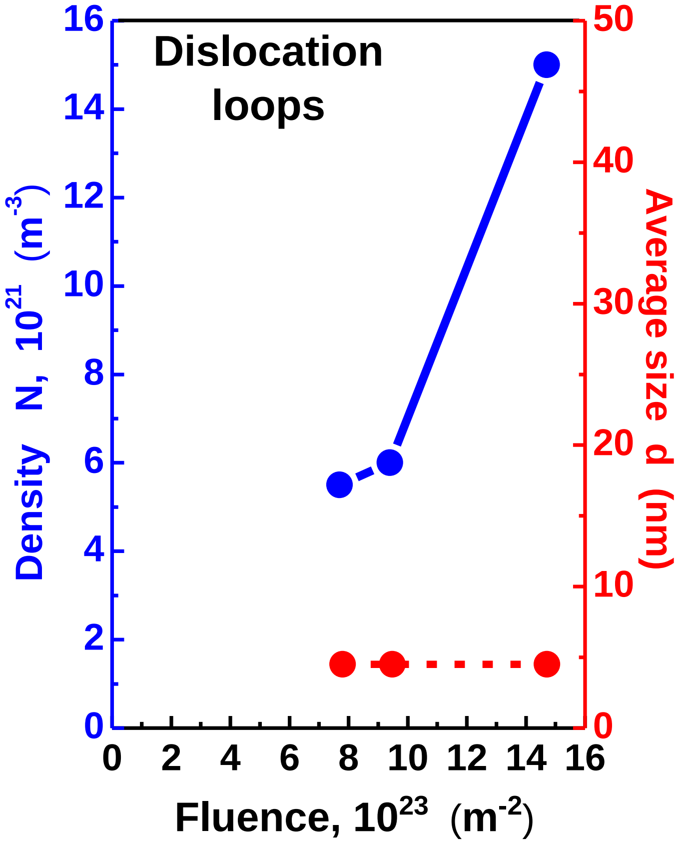

WM (1.77%Ni, 0.74%Mn, 0.26%Si, 0.07%Cu)

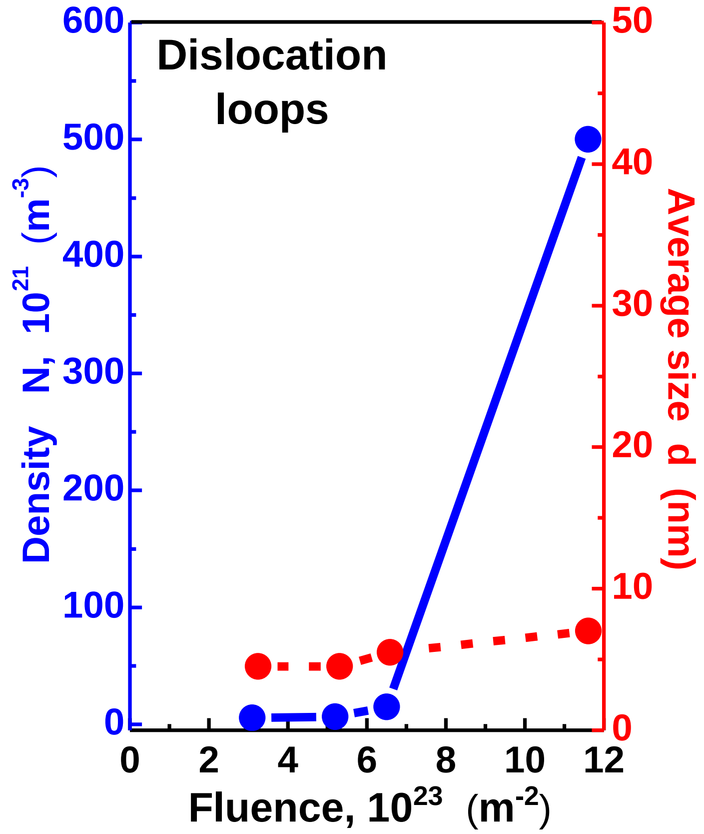

Graphs are built according to the experimental evidence from:
B. A. Gurovich, E. A. Kuleshova, Ya. I. Shtrombakh, D. Yu. Erak, A. A. Chernobaeva, O. O. Zabusov, Journal of Nuclear Materials 389 (2009) 490–496

Brittle strength of irradiated RPV metal

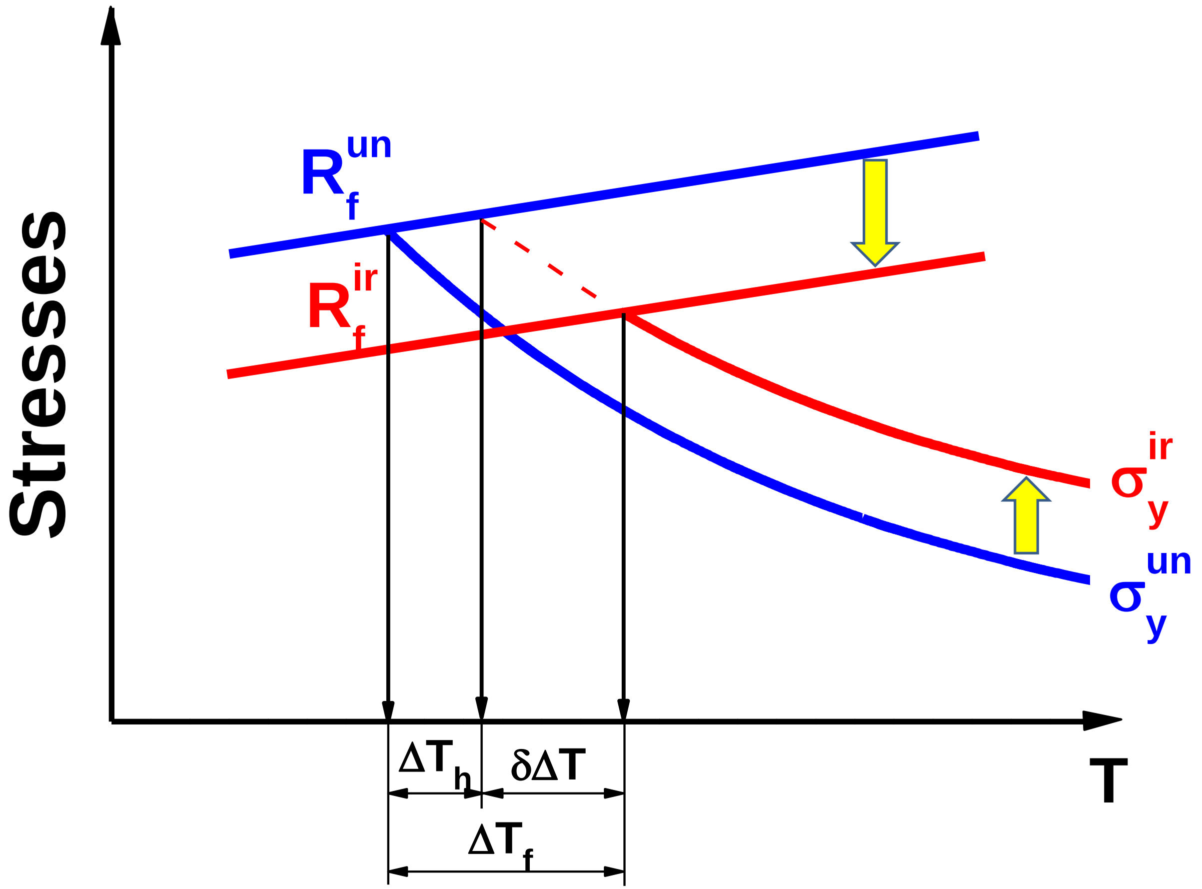

$$\Delta T_f = A_f \times \mathrm{SMFs}(T_{irr}, \varphi t, \mathrm{P}) + B_f \times \mathrm{CRPs}(\mathrm{Cu}, \mathrm{Ni}, \varphi, \varphi t) + \mathrm{LBPs}(?) + \mathbf{C_f} \times \mathbf{\Delta R_f}(\varphi t, ???)$$

Non-hardening embrittlement

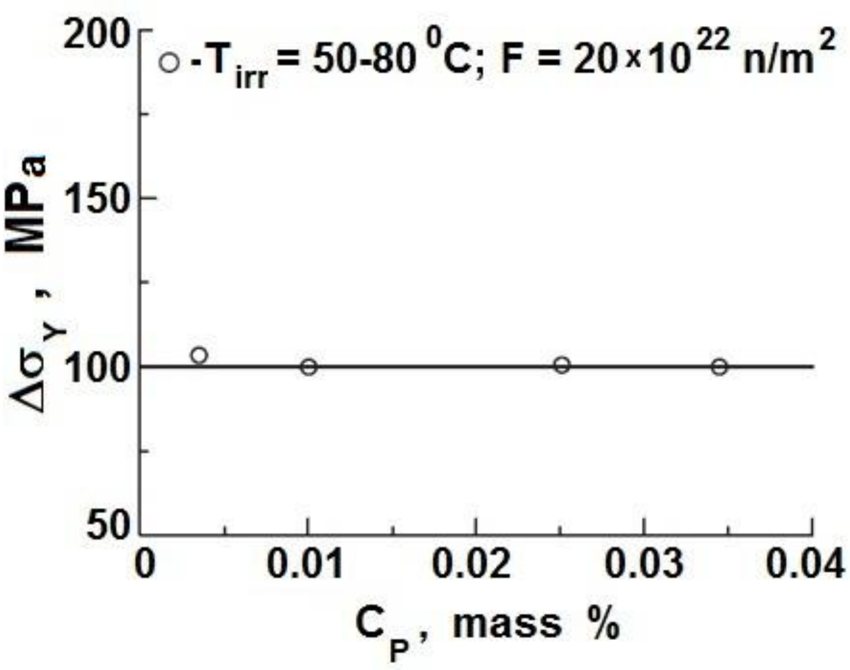

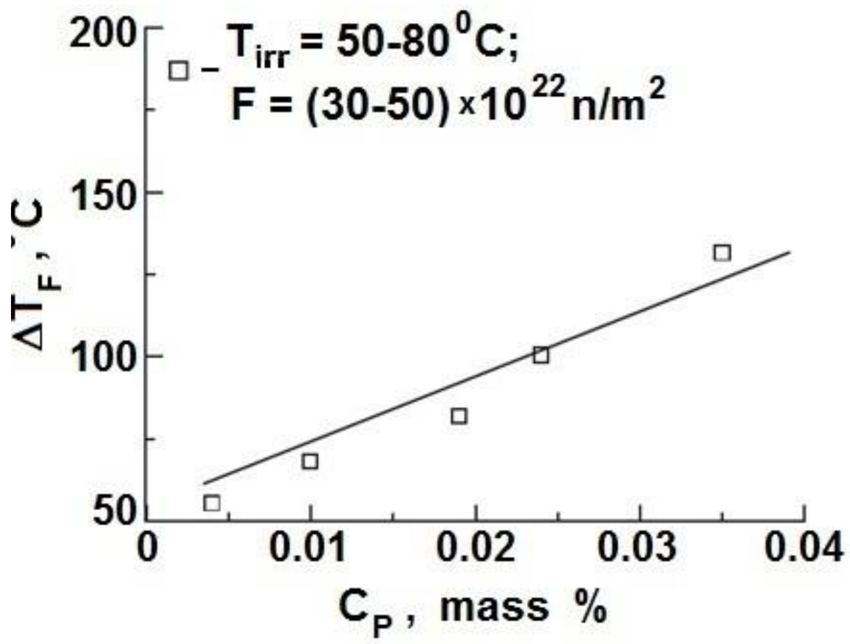

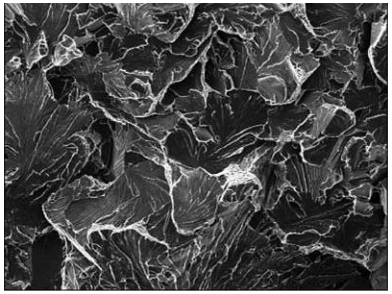

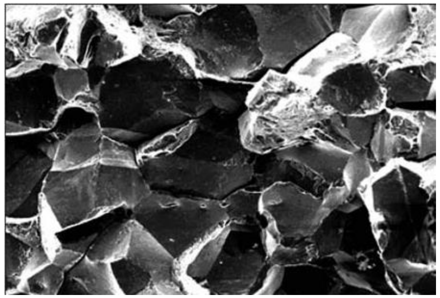

N.N. Alekseenko et al. Radiation damage of nuclear power plant pressure vessel steels, Illinois USA, La Grange Park, 1997.

Assessment of non-hardening mechanism contributions into the ductile-to-brittle transition temperature shifts

Material	Composition, wt.%									
	C	Ni	P	Cu	S	Mn	Si	Cr	Mo	V
Sv-10KhGNMAA	0.06-0.07	1.61-1.89	0.005-0.008	0.03-0.06	0.007-0.019	0.81-0.99	0.29-0.33	1.72-2.01	0.58-0.67	0.01-0.03

State	Fluence, 10^{22}, m^{-2}	Flux, 10^{14}, $m^{-2}\ s^{-1}$	Time, x 1000, h	ΔT_K, ^0C (%)	**Hardening mechanism**	**Non-hardening mechanism**	
					ΔT_F, ^0C / (%)	Thermal part, ^0C (%)	Radiation-enhanced part, ^0C (%)
Initial	---	---	0	---	---	---	---
3d temperature set	---	---	125	23	---	---	---
Irradiation within SS	50	11	125	81	41 (**51%**)	23 (**28%**)	12 (**15%**)

Almost **half** of the transition temperature shift can be caused by the non-hardening mechanism.

It is an artificial "way of" that doesn't enable to determine the value of the brittle strength of irradiated metal and its dependence on the fluence and microstructure.

E. A. Kuleshova et al Journal of Nuclear Materials, Volume 483, January 2017, Pages 1-12

Multiscale Local approach to fracture

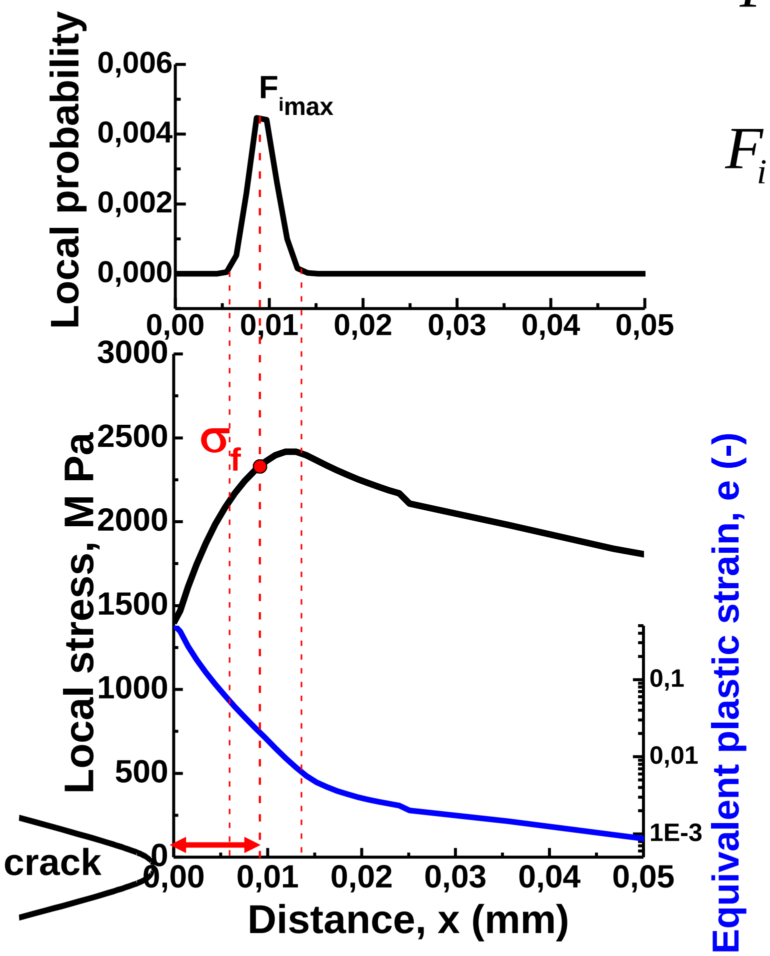

$$F_{\Sigma} = 1 - \prod_{1}^{M} (1 - F_i)$$ - is the probability of **global** fracture;

$$F_i = 1 - [1 - F_0]^{\rho_i V_i}$$ - is the **local fracture probability**.

$$F_0(\sigma_f) = 0.5 \int_{\xi_c^{min}}^{\xi_c^{max}} g(\xi_c) \left[1 - \mathbf{erf}\left(\frac{\xi_c - \sigma_f}{\sqrt{2} I_{\xi} \sigma_f} \right) \right] \mathbf{d}\xi_c$$

$$g(\xi_C) = \frac{2}{k_{Ic}} \int_{\eta_{min}}^{\eta_{max}} g(\eta) \left[\int_{\theta_{min}}^{\theta_{max}} g(\theta) g(a) \frac{a^{3/2}}{\varphi(\theta, \eta)} d\theta \right] \mathbf{d}\eta$$

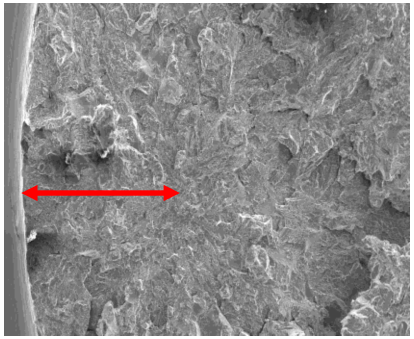

Kotrechko S. Transferability of Fracture Mechanical Characteristic. I. Dlouhy (ed), NATO Science Series. Series II, Vol. 78 (2002), pp.135-150.

Fracture toughness of irradiated steel

Main factors governing the decrease in σ_f and K_{Ic} of irradiated steel:

1**. radiation hardening;**
2. **increase in density of the crack nuclei.**

Weld metal surveillance SENB (0.4T) specimen

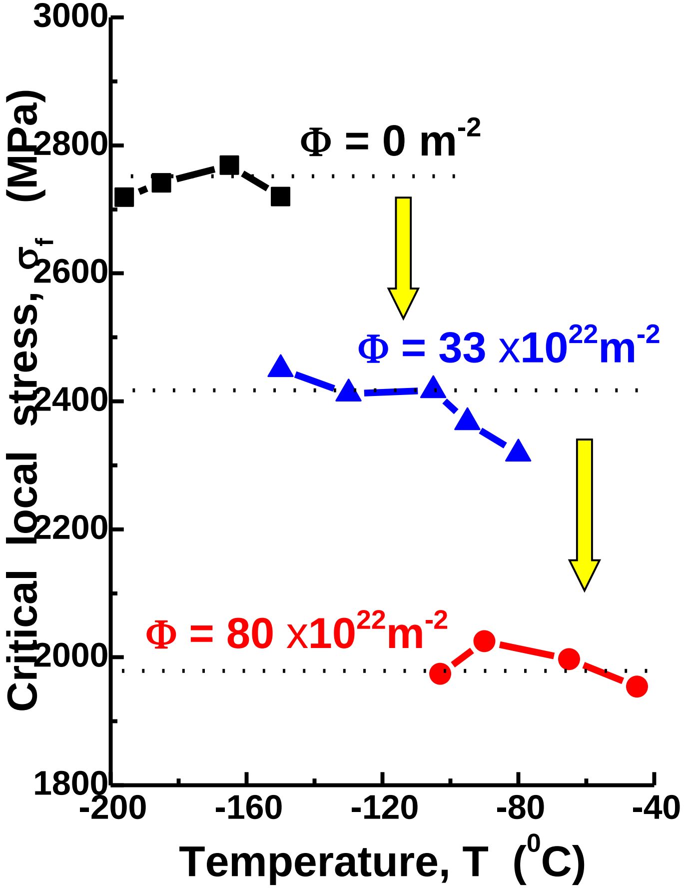

$$\rho \approx \sqrt{\frac{2}{\pi}} k_\rho \int_{t_c}^{t_r} \mathbf{exp}\left(\frac{t^2}{2}\right) dt$$

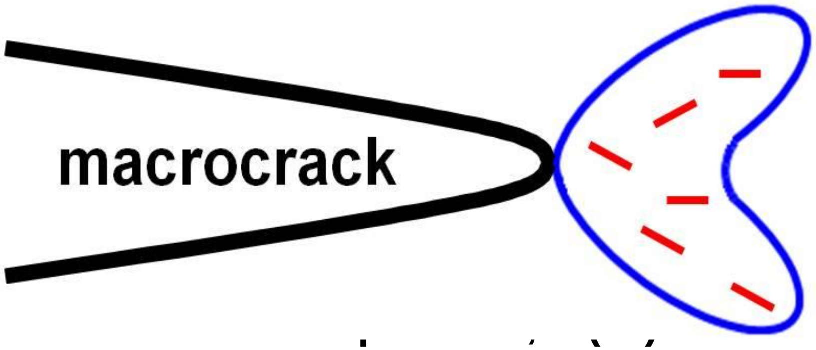

Density of crack nuclei

$$\rho \approx \sqrt{\frac{2}{\pi}} k_\rho \int_{t_c}^{t_r} \mathbf{exp}\left(\frac{t^2}{2}\right) dt$$

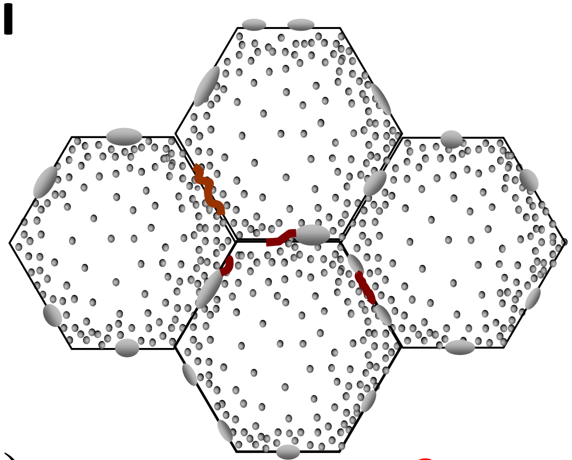

$$t = \frac{\xi_{ns}}{\pm k_\sigma \bar{\bar{\sigma}}}$$ is normalised microstress

$$t_c = \frac{1}{k_\sigma}\left[M + \frac{1}{\bar{\sigma}} \cdot \left(\sqrt{\frac{\tau_C}{CL}} - \beta\sqrt{\frac{\bar{e}}{d}}\right)\right]$$

$$t_r = \frac{1}{k_\sigma}\left[M + \frac{1}{\sigma_i}\left(\frac{\tau_Y}{m}\sqrt{\frac{r}{d_{\mathbf{max}}}} - \beta\sqrt{\frac{e_i}{d}}\right)\right]$$

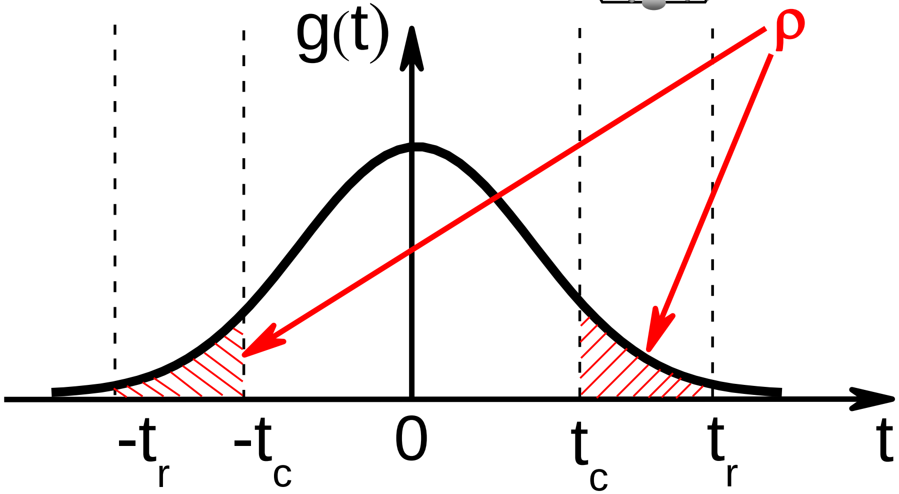

τ_C is critical stress of the crack nucleus formation $\tau_C = f\,(precipitate\ size)$

τ_Y is critical stress of accommodation shears near the grain boundary facets

$$\tau_Y = f\,(precipitate\ \&\ loop\ density,\ \mathbf{P}\text{-}segregation)$$

G.V. Kurdyumov Institute for Metal Physics, NAS of Ukraine
serkotr@gmail.com

Prediction of the end-of-life fluence for the reactor pressure vessel

G.V. Kurdyumov Institute for Metal Physics, NAS of Ukraine
serkotr@gmail.com

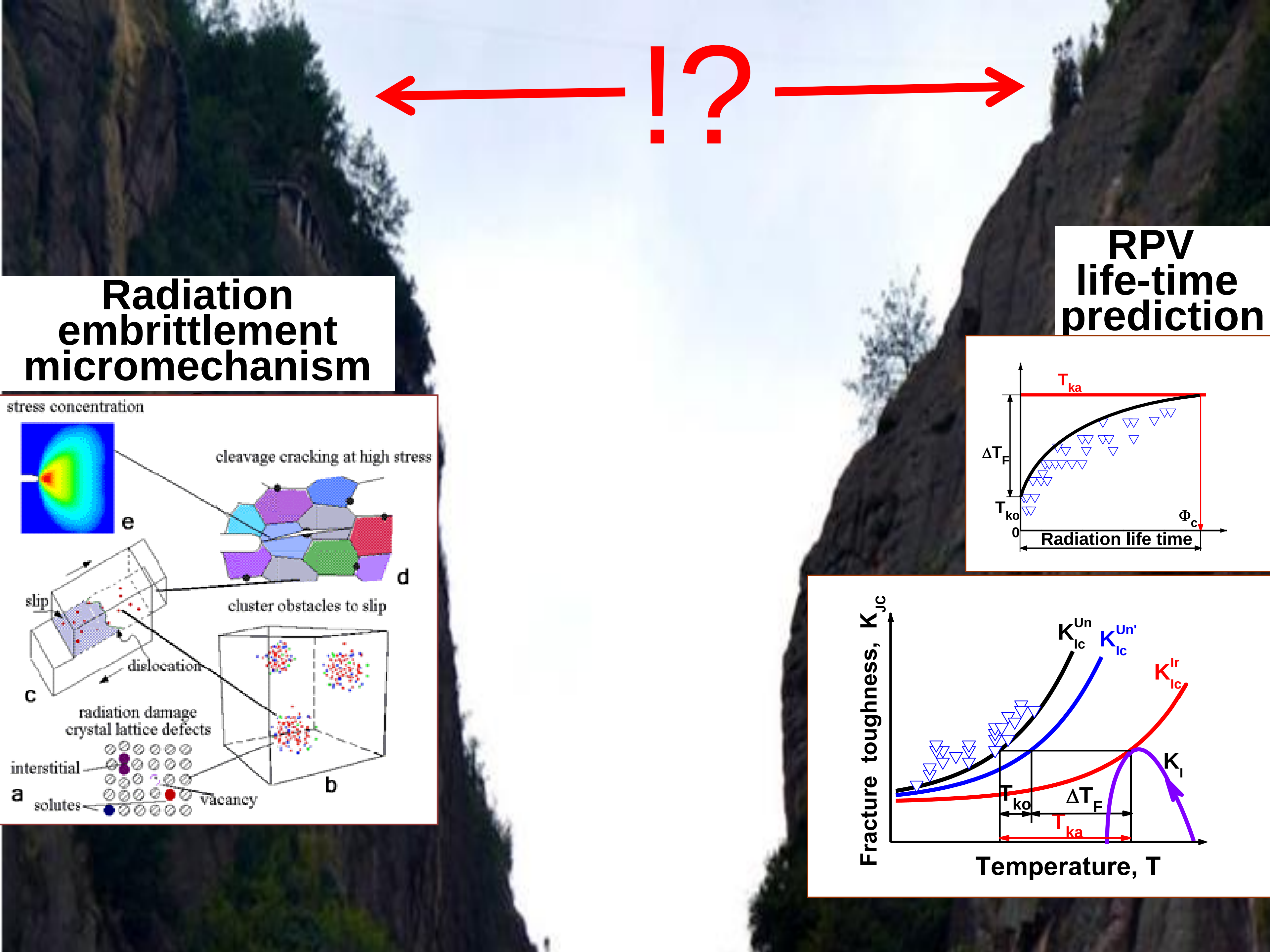
!?
Radiation embrittlement micromechanism
stress concentration
e
cleavage cracking at high stress
d
slip
dislocation
c
cluster obstacles to slip
radiation damage crystal lattice defects
interstitial
vacancy
solutes
a
b
RPV life-time prediction
T_ka
ΔT_F
T_ko
Φ_c
0
Radiation life time
Fracture toughness, K_JC
K_Ic^Un
K_Ic^Un'
K_Ic^Ir
K_I
T_ko
ΔT_F
T_ka
Temperature, T

RPV structural integrity assessment

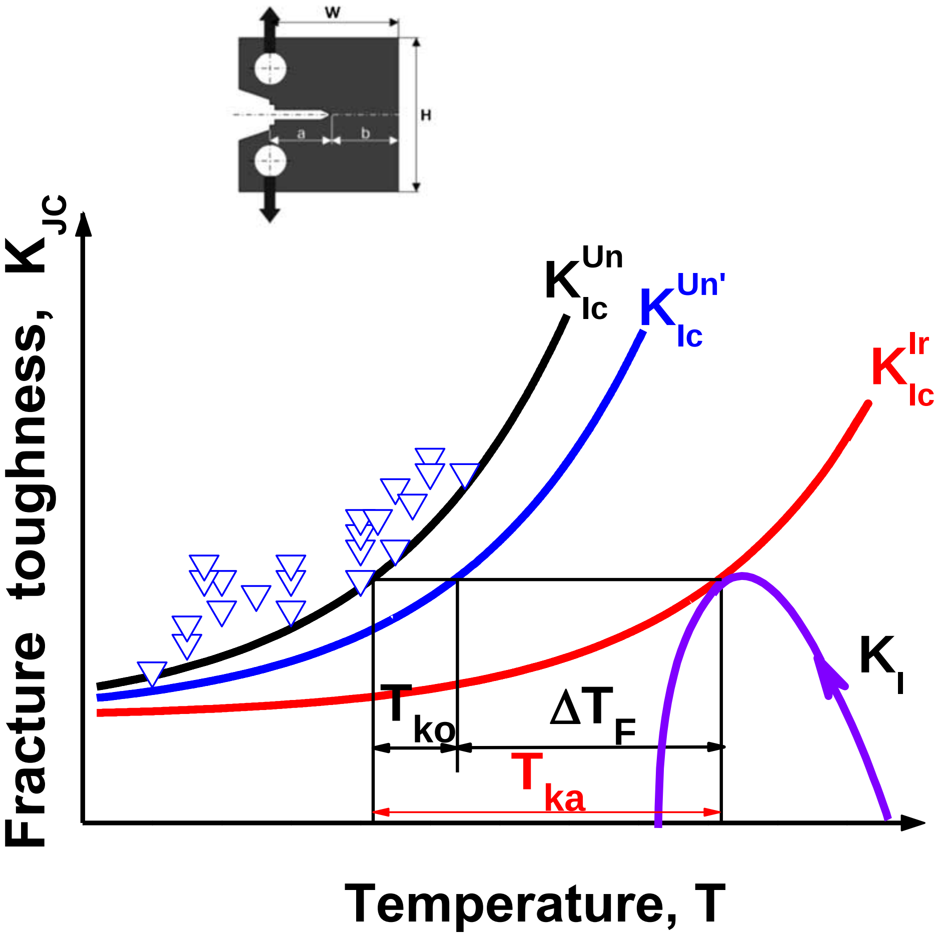

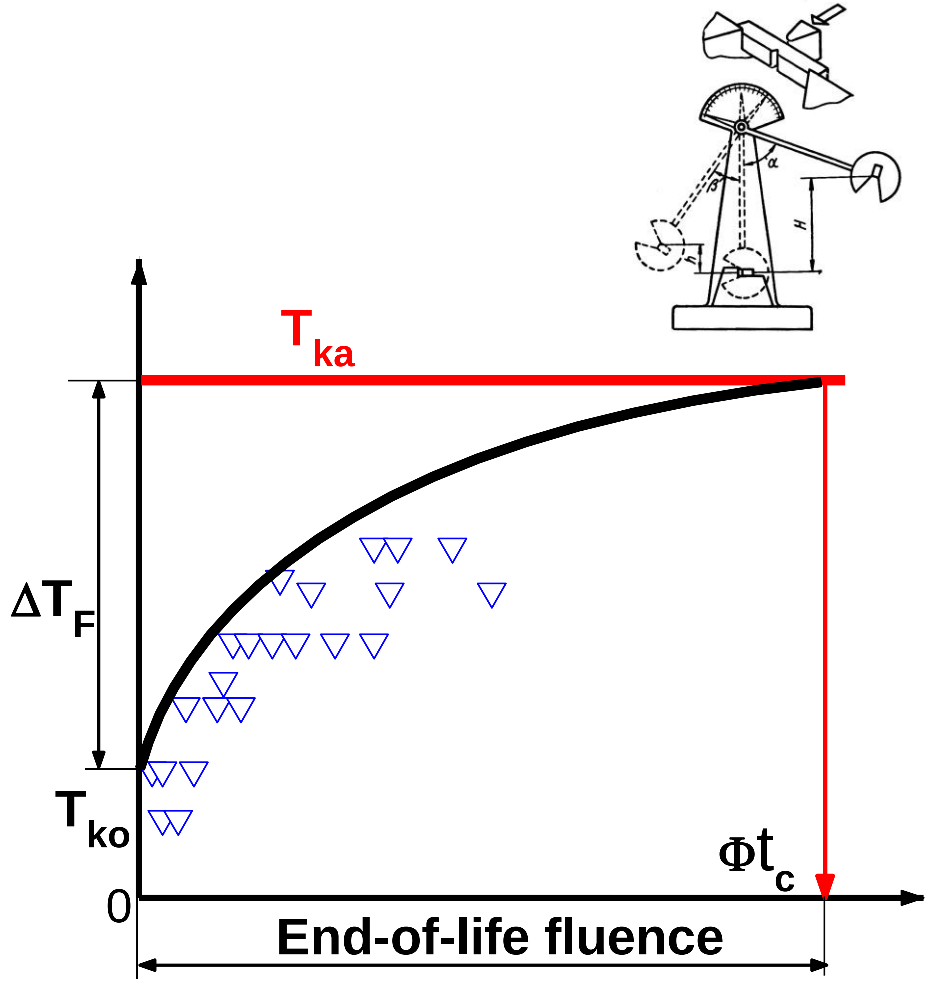

$$\Delta T = A_F (\Phi / \Phi_0)^{1/3} \qquad A_F^{BM} = 23^0 C \qquad A_F^{WM} = 20^0 C$$

Essence of the technique for brittle strength determination

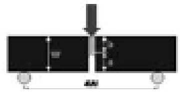

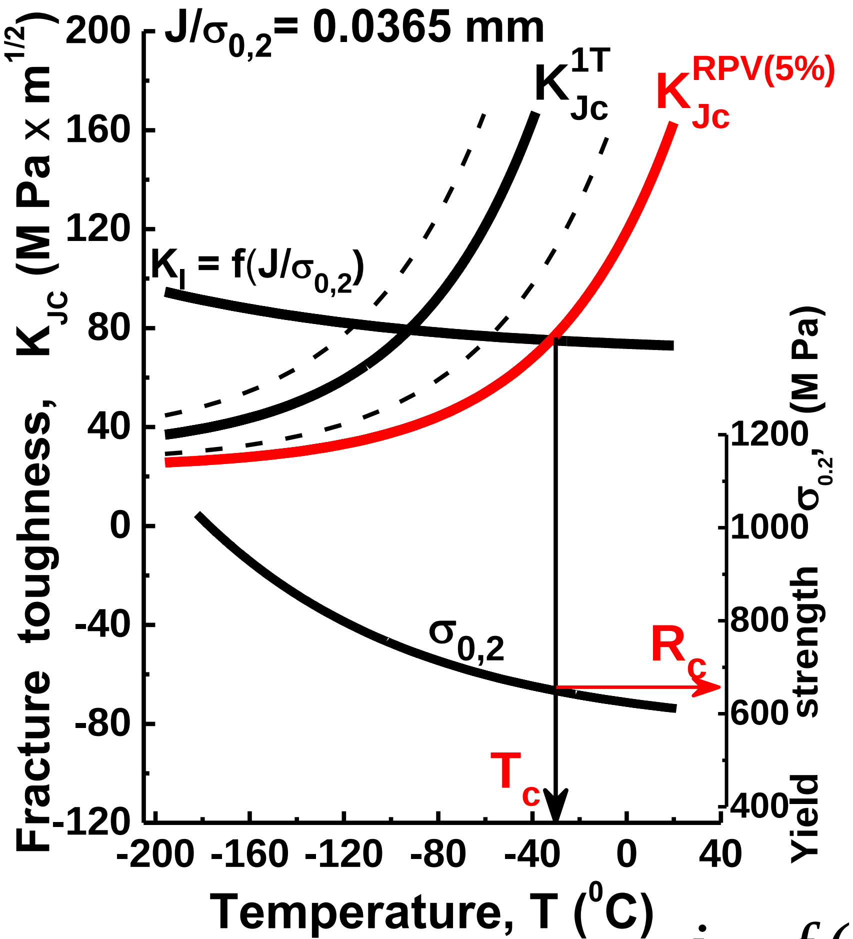

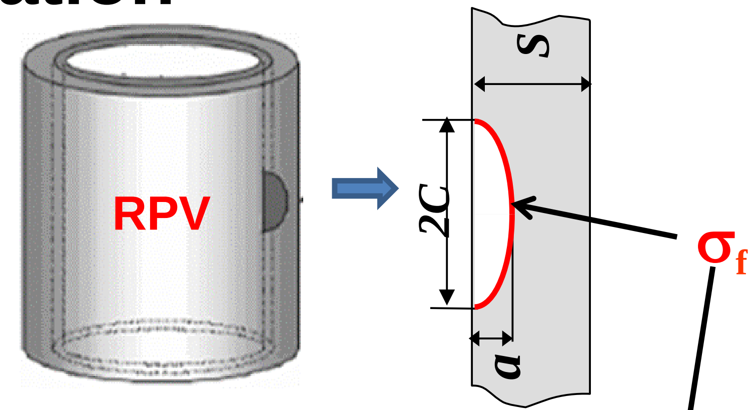

Relation between critical local stress σ_f and brittle strength $\mathbf{R_C}$:

$$R_C \equiv \sigma_{0.2}(T_C) = \frac{\sigma_f}{j}$$

$$j = f(J_I/\sigma_Y)$$

is the overstress factor at the given value of "load" J_I/σ_Y

G.V. Kurdyumov Institute for Metal Physics, NAS of Ukraine
serkotr@gmail.com

Radiation hardening and brittle strength reduction

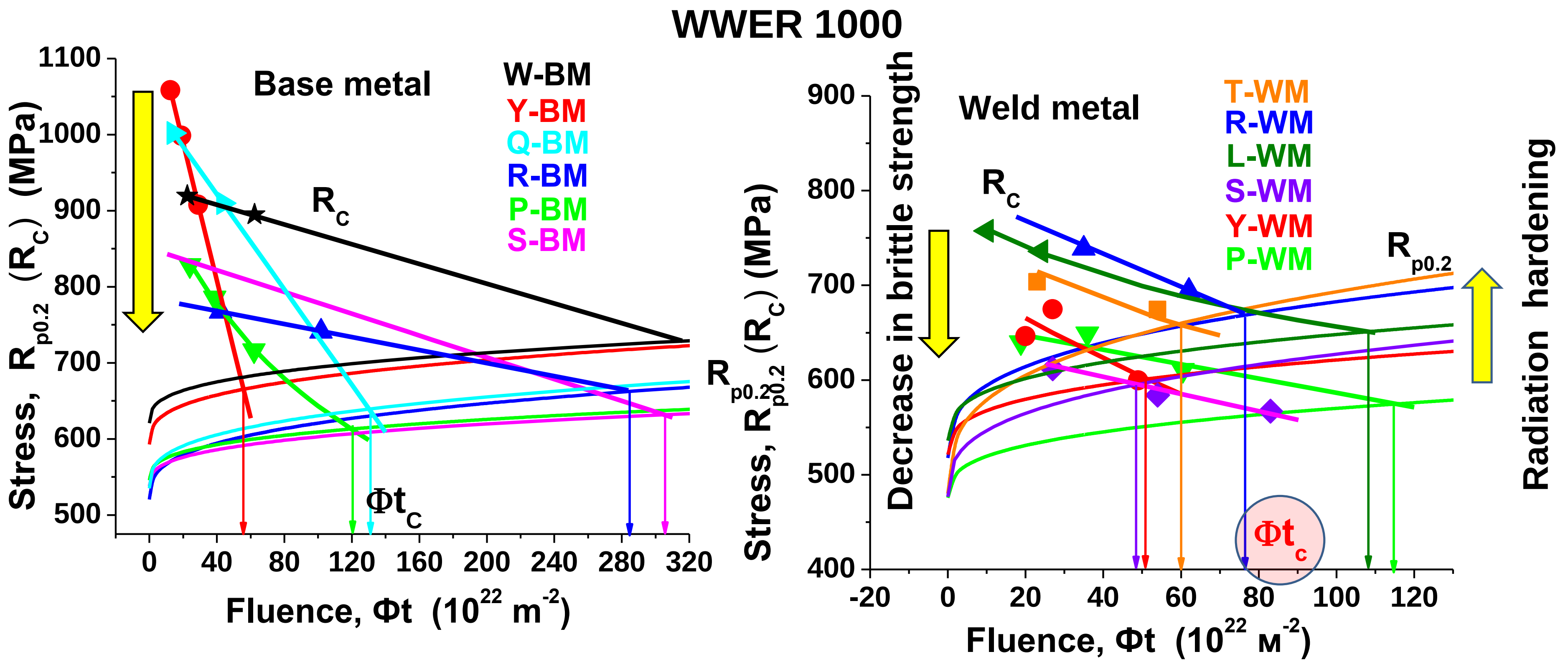

Loading condition:

$J_I/\sigma_{0.2}$ = 0.0365 mm, K_I ~70-75 MPa m$^{0.5}$, T = +56^{0}C

F = 5% failure probability

Postulated crack

a = 25 mm, a/c = 1/3

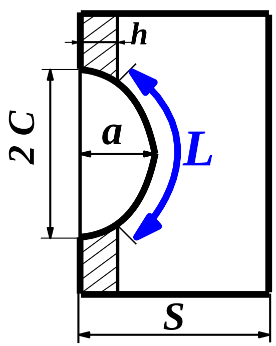

Tests of surveillance specimens were performed in the Institute for Nuclear Researches by Dr. V. Revka and Dr. L. Chyrko.

Engineering Local Approach

Radiation embrittlement micromechanism

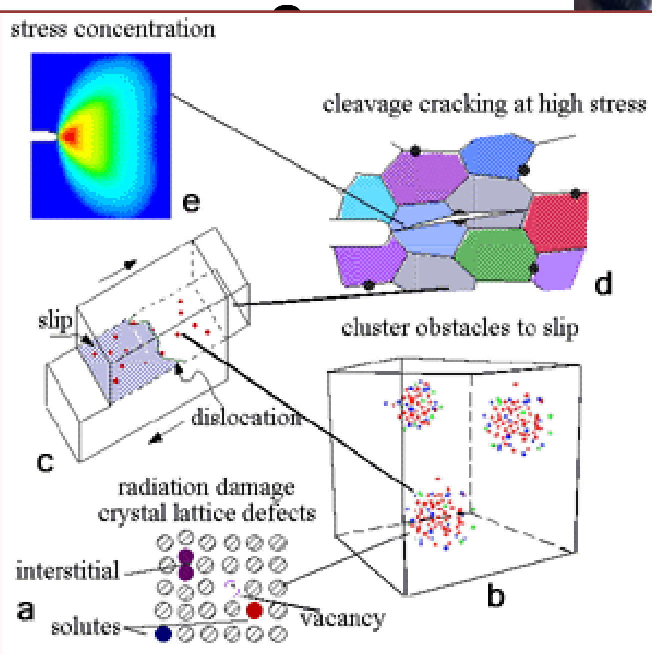

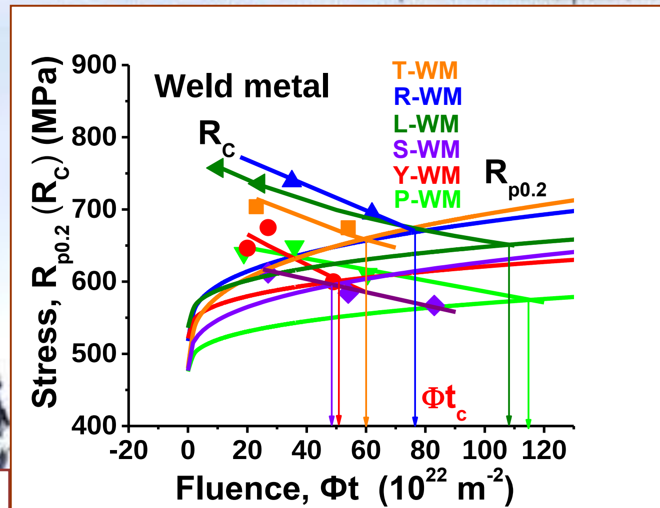

RPV life-time prediction

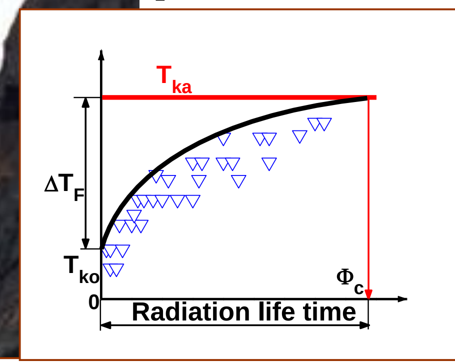

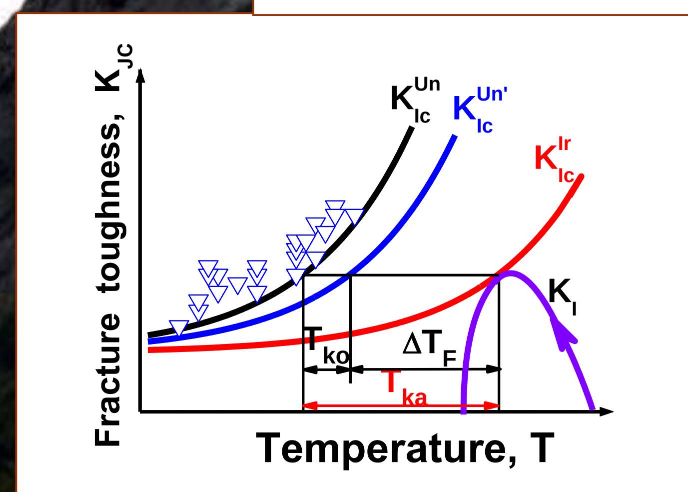

Radiation-induced softening

G.V. Kurdyumov Institute for Metal Physics, NAS of Ukraine
serkotr@gmail.com

In - situ tests

Method of torsional vibrations was used to measure shear modulus.

Shear modulus during irradiation **is lower** than when irradiation is absent at the same values of fluence.

This modulus decrease is fully reversible.

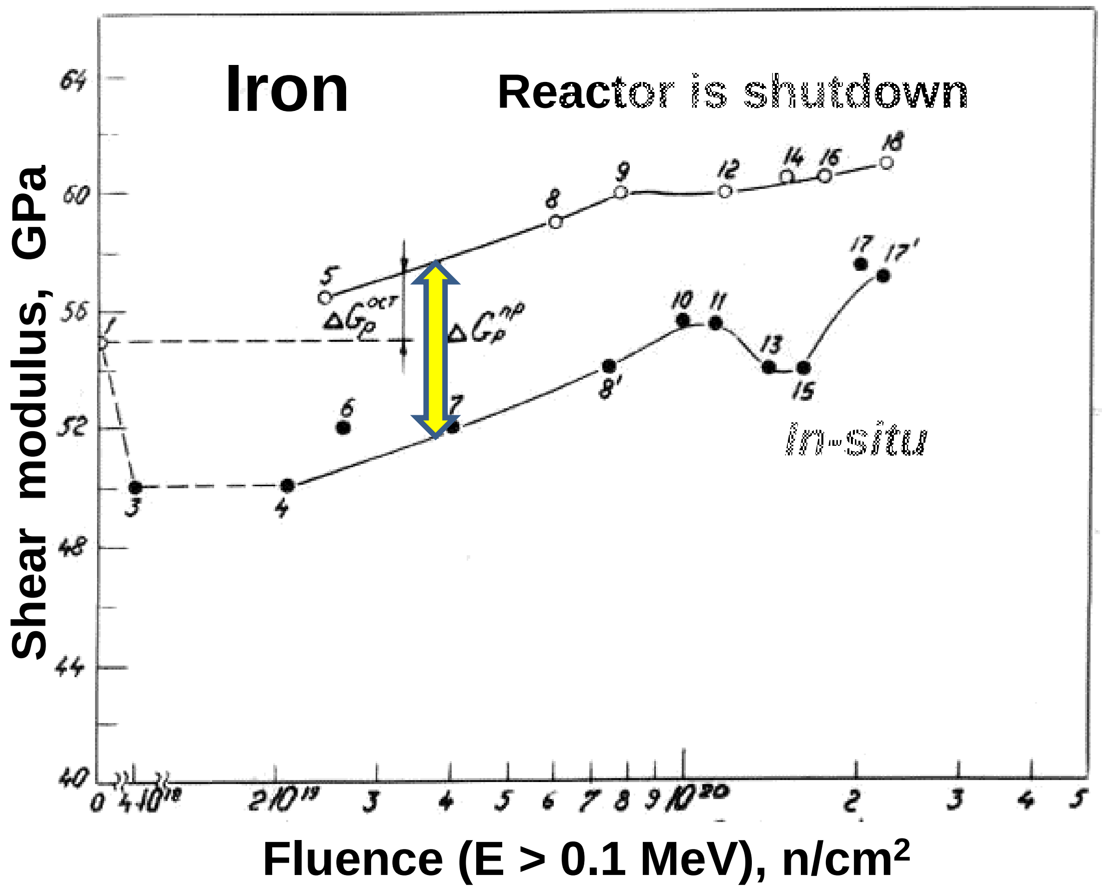

Dependence of G at 580^{0}C on fast neutron fluence (E>0.1 MeV) under *in-situ* irradiation at neutron flux of 10^{18} n/m^{2}s and when a reactor is shutdown.

E. Grynik, V. Karasev, Atomnaya Energiya 54 (1983) 177 (in Russian)

Radiation-induced softening (RIS)

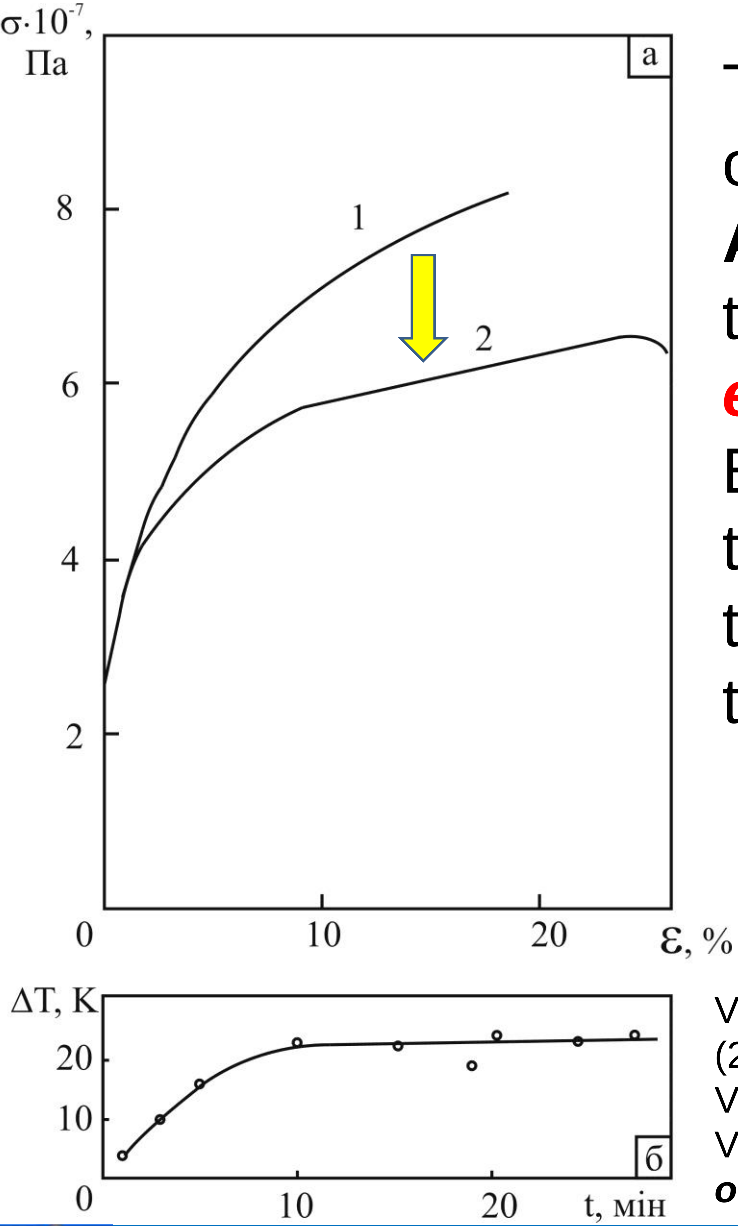

The dependence of the yield stress σ , on the plastic strain ε , of polycrystalline **Al** *without irradiation* at room temperature (the curve 1) and *under* ***electron*** *irradiation* (the curve 2).
Electron energy $0.5\ \mathrm{eV}$,
the beam pulse duration $10^{-6}\ \mathrm{s}$,
the pulse frequency $50\ \mathrm{Hz}$,
the mean electron flux $5\times10^{17}\ \mathrm{e}\times\mathrm{m}^{-2}\times\mathrm{s}^{-1}$

Slide courtesy of Dr. V. Dubinko

V. I. Dubinko, P. A. Selyshchev, and J. F. R. Archilla, ***Phys. Rev.*** E 83 (2011) No 4
V. I. Dubinko, A.N. Dovbnya, V. A. Kushnir, I. V. Khodak, V.P. Lebedev, V.S. Krylovskiy, S.V. Lebedev, V.F. Klepikov, P. N. Ostapchuk, ***Physics of the solid state*** 54 (2012) #12, p. 2442

Calculated hardening of Fe due to dislocation loop formation *under* different neutron fluxes compared to the hardening *after* irradiation at neutron flux of 8×10^{18} m^{-2} s^{-1}

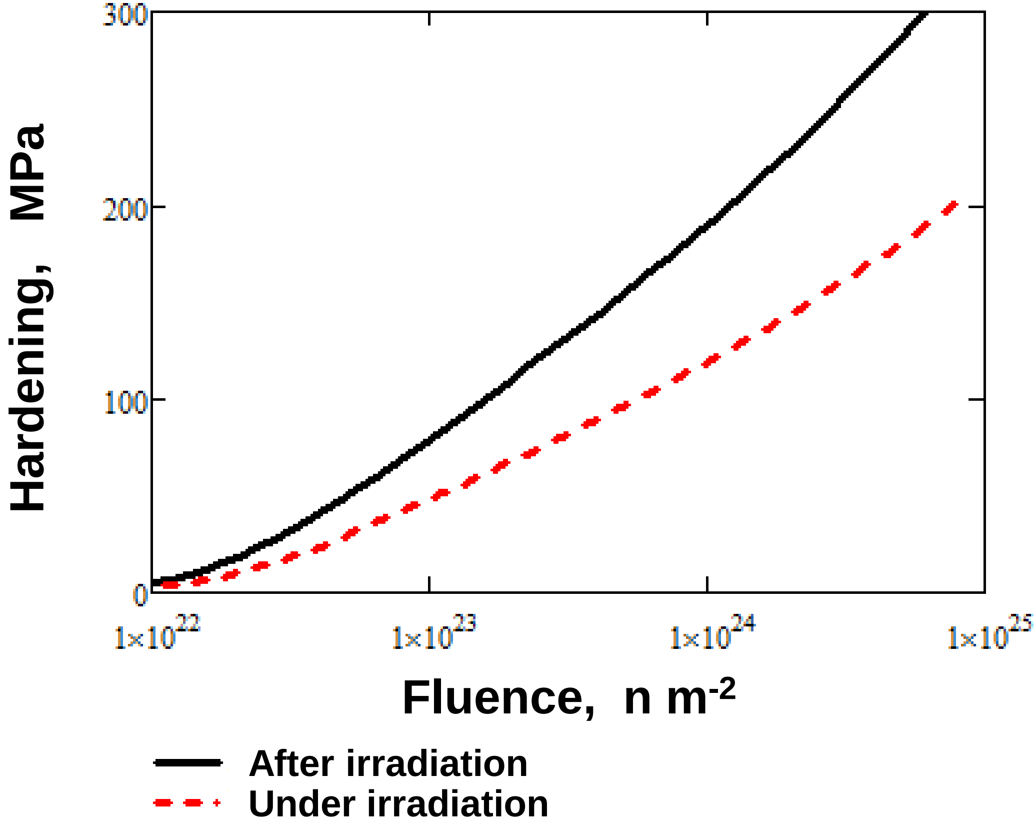

Slide courtesy of Dr. V. Dubinko

Conclusions and Open Issues (OI)

1. In RPV steels, dislocation loops can be "fixed" by segregated atoms, therefore, when assessing radiation hardening, they should be considered as "strong obstacles“.
2. In theoretical and experimental studies of MN precipitates, it is necessary to take into account the interrelation between the kinetics of their formation and the kinetics of formation of dislocation loops.

OI. Development of advanced models of radiation hardening accounting for both the properties of individual defects and the collective processes of interaction of a moving dislocation with a field of defects.

G.V. Kurdyumov Institute for Metal Physics, NAS of Ukraine
serkotr@gmail.com

Conclusions and Open Issues (OI)

3. Until now, there are controversial viewpoints on the existence or not of “Late blooming phases” and whether they a really “blooming” or not.

   Increase in the number density of Ni-Si-Mn-enriched nano-clusters was observed in WWER-1000 base metal and high-Ni weld metal, however, these clusters are neither “late” nor “blooming”. Therefore, accelerated radiation hardening should be considered as necessary, but not sufficient attribute of Late Blooming effect.

OI. Critical analysis and identification of the conditions, at which unexpectedly severe hardening or embrittlement occurs.

Conclusions and Open Issues (OI)

4. Along with radiation hardening, decreasing in **brittle strength** under neutron irradiation has a **significant effect** on the radiation embrittlement of RPV steels.

OI. Transition from purely engineering empirical methods of the RPV lifetime prediction to methods based on realistic physical models of radiation embrittlement of metal taking into account both radiation hardening and reduction in **brittle strength**.

OI. Experimental verification of radiation-induced softening effect for RPV steels under neutron irradiation, and assessment of its effect on the service time of RPV.

G.V. Kurdyumov Institute for Metal Physics, NAS of Ukraine
serkotr@gmail.com

Acknowledgments

I wish to express my sincere appreciation to my colleagues for their assistance in preparing this presentation:

Dr. Vladimir Revka
Dr. Vladimir Dubinko
Dr. Nataliya Stetsenko
Dr. Oleksandra Zatsarna
Research associate Galyna Zimina
Engineer Oksana Shamis

G.V. Kurdyumov Institute for Metal Physics, NAS of Ukraine
serkotr@gmail.com

Thank you for your attention!!!

serkotr@gmail.com

TABLE 14. IRRADIATION-INDUCED DEFECTS IN RPV STEELS

Type	Radius (nm) / Number density	Composition
Copper-rich precipitates	0.5–1.5 nm / some 10^{24} m^{-3}	Cu (>50%) — Mn–Ni–Si
Manganese nickel-rich precipitates	Similar to copper rich precipitates	Mn–Ni–Si (>50%) — Cu
Dilute solute atmospheres	<2 nm / <10^{24} m^{-3}	Fe–Cu–Mn–Ni–Si
Vacancy-solute clusters	<0.5–1.5 nm / <10^{24} m^{-3}	Vacancies — Cu–Mn–Ni–Si
Nanovoids	<0.5 nm / <10^{24} m^{-3}	Vacancies — Cu–Mn–Ni–Si
SIA clusters	<0.3 nm / some 10^{24} m^{-3}	—
SIA dislocation loops	<0.8 nm / some 10^{24} m^{-3}	—

serkotr@gmail.com

Table 1
Chemical composition of the investigated VVER-1000 base and weld materials.

Element	Base metal		Weld metal	
Balance Fe	wt%	at.%	wt%	at.%
C	0.17	0.78	0.08	0.28
Si	0.29	0.59	0.26	0.65
Mn	0.47	0.46	0.74	0.81
Cr	2.24	2.34	1.80	1.93
Ni	1.34	1.19	1.77	1.69
Cu	0.05	0.04	0.07	0.06
S	0.014	0.024	0.013	0.023
P	0.009	0.014	0.006	0.009
V	0.09	0.11	0.02	0.02
Mo	0.51	0.30	0.64	0.33

WESTERN - Since 1970s, C phosphorus concentration maximum value of 0.015% and, later, even lower values, in most Western countries (e.g. 0.008% in France)

Local approach to cleavage fracture

Local fracture probability, F_i

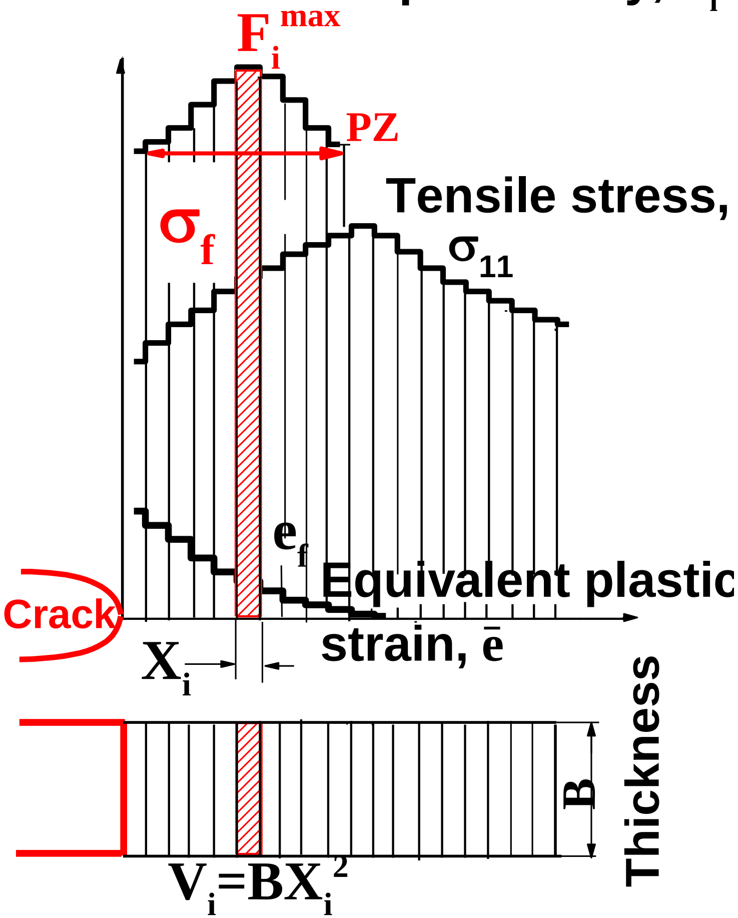

BEREMIN Local approach:

P_F is global fracture probability;

$$P_F = 1 - \mathbf{exp}\left[-\int_{PZ}\left(\frac{\sigma_1}{\sigma_u}\right)^m \frac{dV}{V_0}\right]$$

$$m = f(\Phi t) \qquad \sigma_u = f(\Phi t)$$

"Prometey" Local approach:

$$\sigma_1 \geq S_C(\varpi)$$

$$\sigma_1 + m_{T_\varepsilon} \cdot \sigma_{eff} \geq \sigma_d$$

$$\sigma_d = f(\Phi t)$$

Beremin F., *Metallurgical Transactions,* 1983 *A 14, 2277-2287*

B.Z. Margolin, V.A. Shvetsova, A.G. Gulenko, V.I. Kostylev
International Journal of Pressure Vessels and Piping 2007, 84 320–336

Tensile strength of smooth (unnotched) specimens

“Local” scale effect

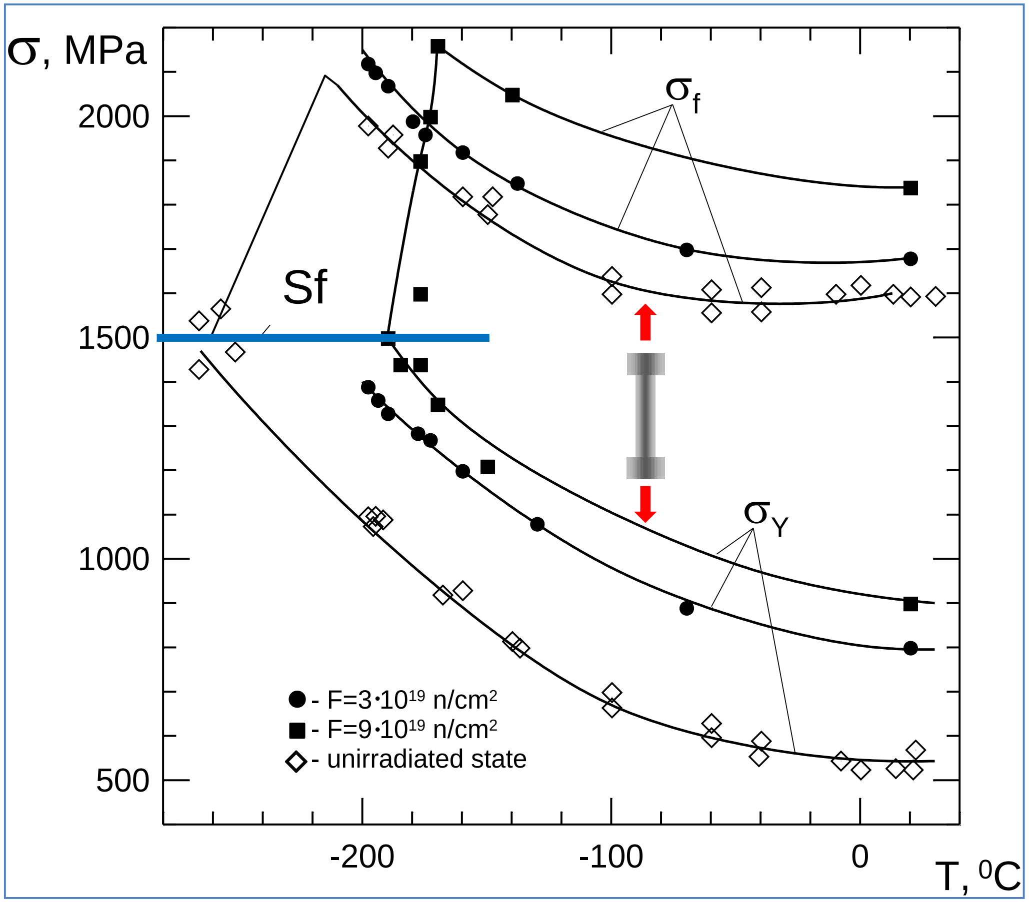

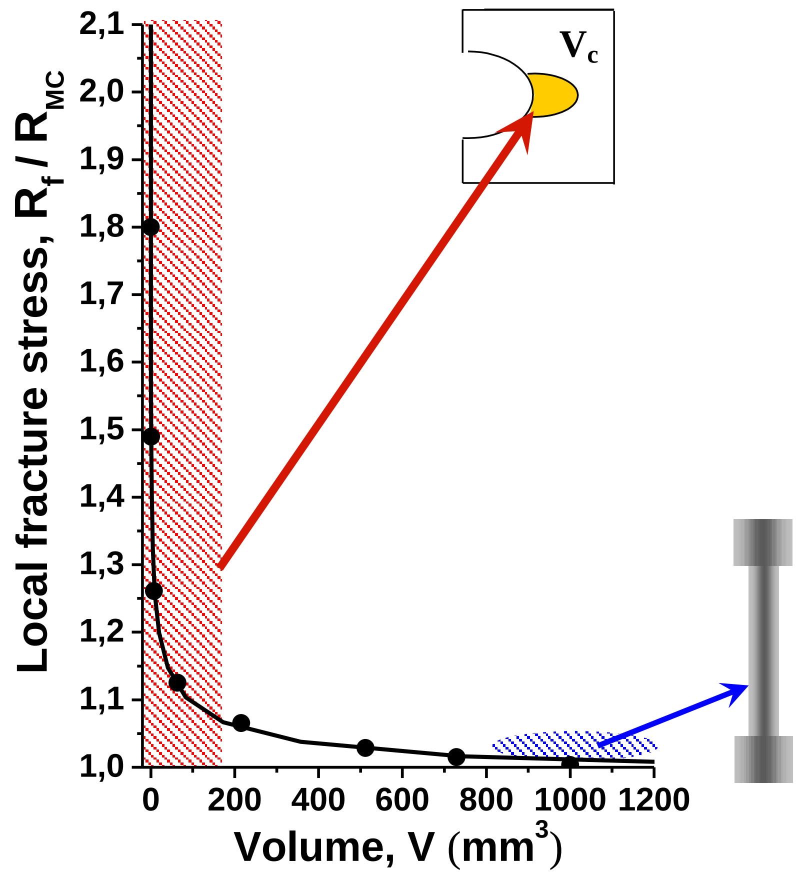

Viner et al., 1971; RPV-440 base metal

Relation between radiation hardening and microstructure features

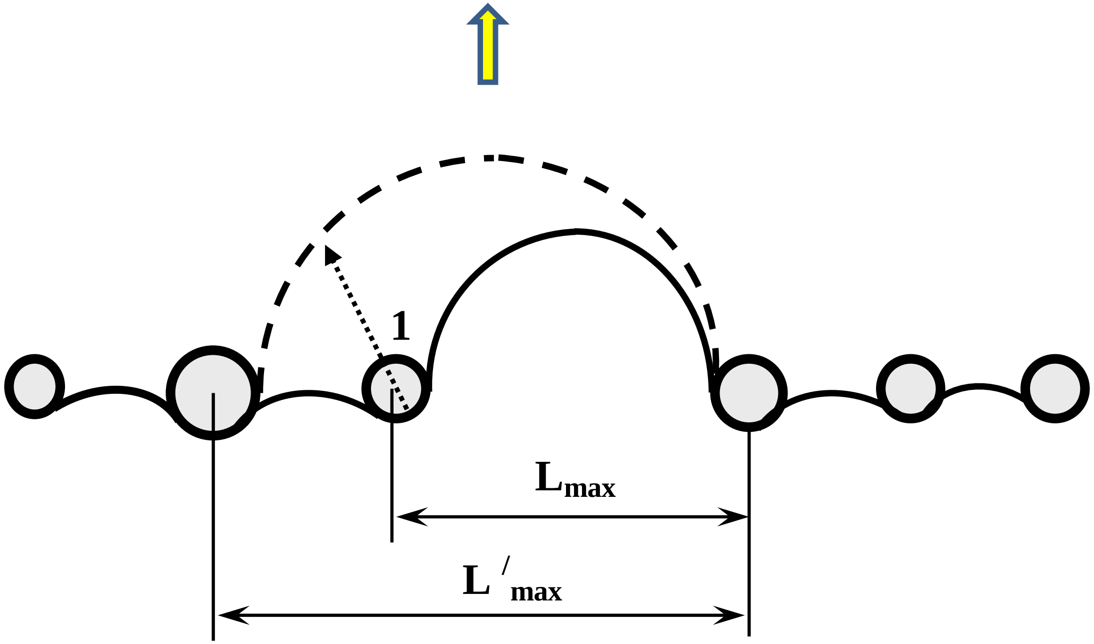

"Orowan mechanism":

$$\Delta\sigma_Y = \alpha M G b \times \sqrt{Nd}$$

α is the obstacle strength

N is the number density

d is the diameter

Precipitate shearing:

$$\Delta\sigma_Y = \gamma \cdot \frac{0.81\pi M}{8b} \times d\sqrt{dN}$$

D. N. Seidman, E. A. Marquis, D. C. Dunand, Acta Materialia 50 (2002) 4021–4035

Orowan dependence for the wide range of change in fluences

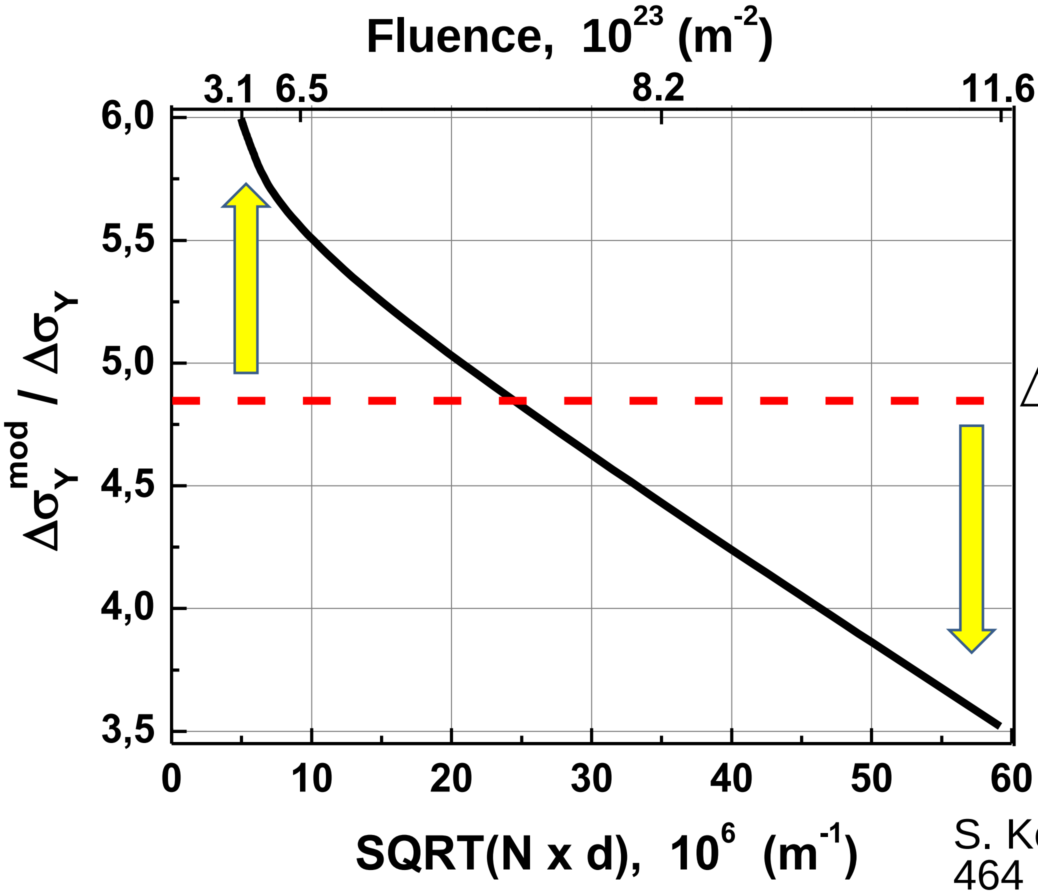

Conventional version:

$$\Delta\sigma_Y = \alpha M G b \times \sqrt{Nd}$$

Modified version:

$$\Delta\sigma_Y^{mod} = 0.85\alpha_0 \frac{F}{2\pi} M G b \times \boldsymbol{f(N,d)}$$

$$\boldsymbol{f(N,d)} = \mathbf{ln}\left(\frac{1}{2b\sqrt{Nd}}\right) \times \sqrt{Nd}$$

is the structural function

S. Kotrechko et. al, Journal of Nuclear Materials 464 (2015) 6–15

Graph is built according to the experimental evidence from:

B.A. Gurovich, E.A. Kuleshova, Ya.I. Shtrombakh, D.Yu. Erak, A.A. Chernobaeva , O.O. Zabusov Journal of Nuclear Materials 389 (2009) 490–496

Material – WWER-1000 WM (Ni=1.77%, Mn= 0.74%, Si=0.26%, Cu=0.07%, P=0.006%)

Change in the dominant hardening micromechanism

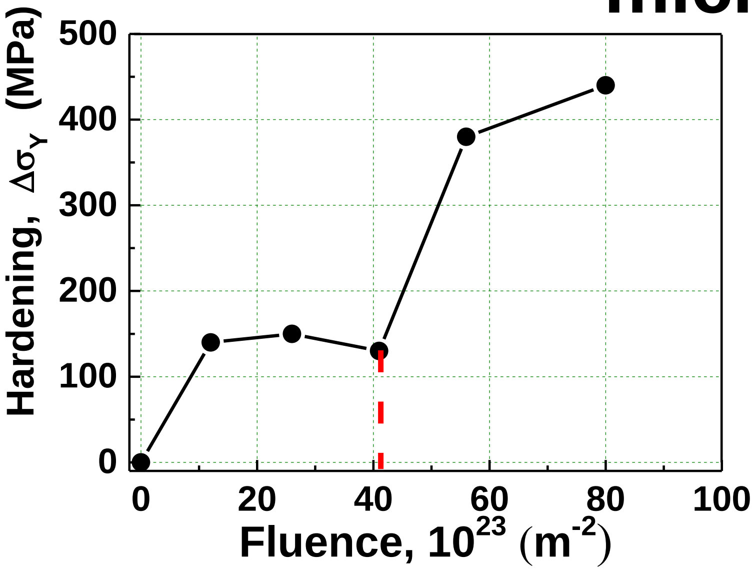

$$\Delta\sigma_Y = 0.85\frac{F}{2\pi}\cdot\alpha_0 MGb\times \boldsymbol{f(N,d)}$$

$$\boldsymbol{f(N,d)} = \mathbf{ln}\left(\frac{1}{2b\sqrt{Nd}}\right)\times\sqrt{Nd}$$

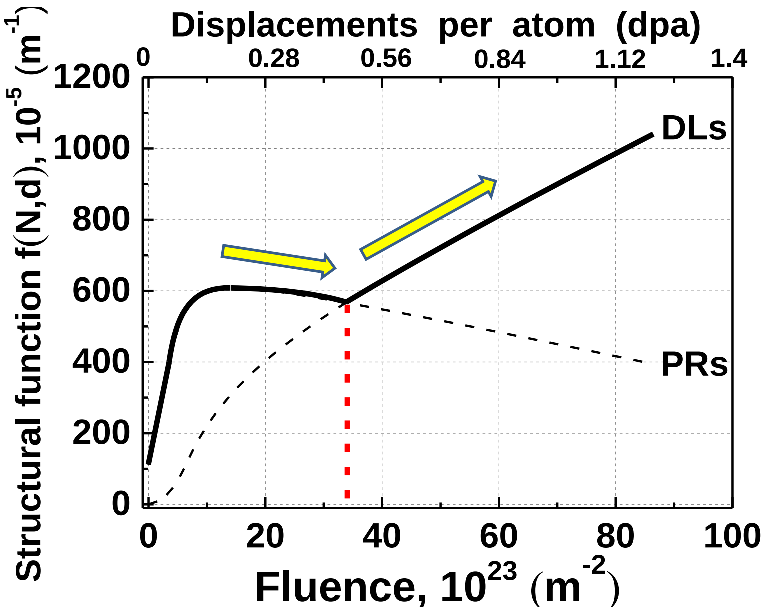

WWER-440: weld metal Sv-10KhMFT

Chemical composition of the material studied (wt%):

C	Si	Mn	P	Cu
0.05	0.29	0.87	0.010	0.03

Graphs are built according to the experimental evidence from:

E. A. Kuleshova, B. A. Gurovich, Ya. I. Shtrombakh, Yu. A. Nikolaev, V. A. Pechenkin, Journal of Nuclear Materials 342 (2005) 77–89.